Acta Pharmacologica Sinica 2017: 1353–1368
 1671-4083/17
www.nature.com/aps

Original Article

Synthesis and *in vitro* biological evaluation of thiosulfinate derivatives for the treatment of human multidrug-resistant breast cancer

Ariane ROSEBLADE[1], Alison UNG[2], Mary BEBAWY[1, *]

[1]*Discipline of Pharmacy, Graduate School of Health, The University of Technology Sydney, Sydney, NSW, Australia;* [2]*School of Mathematical and Physical Sciences, Faculty of Science, The University of Technology Sydney, Sydney, NSW, Australia*

Abstract

Organosulfur compounds derived from *Allium* vegetables have long been recognized for various therapeutic effects, including anticancer activity. Allicin, one of the main biologically active components of garlic, shows promise as an anticancer agent; however, instability makes it unsuitable for clinical application. The aim of this study was to investigate the effect of stabilized allicin derivatives on human breast cancer cells *in vitro*. In this study, a total of 22 stabilized thiosulfinate derivatives were synthesized and screened for their *in vitro* antiproliferative activities against drug-sensitive (MCF-7) and multidrug-resistant (MCF-7/Dx) human adenocarcinoma breast cancer cells. Assays for cell death, apoptosis, cell cycle progression and mitochondrial bioenergetic function were performed. Seven compounds (**4b**, **7b**, **8b**, **13b**, **14b**, **15b** and **18b**) showed greater antiproliferative activity against MCF-7/Dx cells than allicin. These compounds were also selective towards multidrug-resistant (MDR) cells, a consequence attributed to collateral sensitivity. Among them, **13b** exhibited the greatest anticancer activity in both MCF-7/Dx and MCF-7 cells, with IC_{50} values of 18.54±0.24 and 46.50±1.98 μmol/L, respectively. **13b** altered cellular morphology and arrested the cell cycle at the G_2/M phase. Additionally, **13b** dose-dependently induced apoptosis, and inhibited cellular mitochondrial respiration in cells at rest and under stress. MDR presents a significant obstacle to the successful treatment of cancer clinically. These results demonstrate that thiosulfinate derivatives have potential as novel anticancer agents and may offer new therapeutic strategies for the treatment of chemoresistant cancers.

Keywords: garlic; allicin; thiosulfinate derivatives; breast cancer; multidrug resistance; cell cycle arrest; apoptosis; mitochondrial respiration

Acta Pharmacologica Sinica (2017) 38: 1353–1368; doi: 10.1038/aps.2016.170; published online 31 Aug 2017

Introduction

Cancer is one of the primary causes of mortality worldwide, accounting for approximately 8 million deaths per year[1]. While significant advances in diagnostic screening, surgical resection, and targeted therapies have been made in recent years, many types of malignancy remain difficult to cure. Currently, the most common forms of treatment include radiotherapy, surgery and chemotherapy; however, resistance to chemotherapy, whether intrinsic or acquired, presents a significant obstacle to the successful treatment of cancer.

Multidrug resistance (MDR) occurs when cancer cells become cross-resistant to a wide variety of structurally and functionally unrelated drugs and is predominately associated with increased expression of multidrug efflux transporters in the cell membrane, such as P-glycoprotein (P-gp)[2, 3]. P-gp facilitates ATP-dependent efflux of chemotherapeutic drugs, allowing MDR cells to maintain sub-lethal intracellular concentrations of these compounds, resulting in poor therapeutic response and prognosis in many types of cancer[4–6]. A broad range of synthetic and natural P-gp inhibitors have been investigated, but due to lack of efficacy and dose-limiting toxicity, these have so far proven to be unsuitable for clinical application[7].

Phytochemicals have long been known to have numerous health benefits in addition to showing potential as anticancer agents and modulators of MDR[8–10]. Organosulfur compounds derived from *Allium* vegetables, such as onion (*Allium cepa*) and garlic (*Allium sativum*), are well documented as having a wide range of protective effects in numerous disease states. The consumption of these vegetables is associated with many health benefits, including a reduced risk of cancer[11–14].

Allicin, an allyl thiosulfinate, is the main biologically active

*To whom correspondence should be addressed.
E-mail mary.bebawy@uts.edu.au
Received 2016-09-12 Accepted 2016-12-21

compound derived from garlic, and it has been shown to exhibit various biological effects including antioxidant[15], antiparasitic[16, 17], antimicrobial[18], antibacterial[19], anti-inflammatory[20, 21], and anticancer activity[22–24]. *In vitro* studies have shown that allicin inhibits cancer cell proliferation through cell cycle arrest in gastric, breast and cervical cancer[25–27]. Studies have also shown that allicin induces apoptosis in leukemia-derived cells through the depletion of cellular glutathione (GSH) and modulation of the cellular redox state[28], as well as significantly increasing reactive oxygen species (ROS) production in liver cancer, leading to reduced mitochondrial membrane potential, apoptosis, and cell death[29]. Additionally, allicin and saturated short-chain thiosulfinate analogs are known to act on intracellular calpain, inhibiting invasion and migration in cancer cells[30]. This activity inhibits the release of microparticles (MPs), which have been shown to transfer P-gp from MDR cells to drug-sensitive cells[31, 32]. These findings make these compounds attractive leads in targeting proliferation, metastasis and MDR in cancer[30, 32–34]. Importantly, allicin and thiosulfinate derivatives have been shown to be cancer-specific while being non-toxic to normal cells and have been reported to increase survival times in tumor-bearing mice[35, 36].

The anticancer activity of allicin is widely attributed to the allylthio group; however, this group is highly unstable, and as a consequence, allicin is prone to decomposition under relatively mild conditions[37–39]. To circumvent this instability and to increase potency and compound half-life, substitution of the labile allylthio group with saturated alkanes and/or benzyl moieties has been shown to prevent thiosulfinate degradation in storage and under biological conditions[39, 40].

In the present work, we describe the synthesis and anticancer activity of a series of aromatic and aliphatic thiosulfinates against both the human adenocarcinoma breast cancer cell line MCF-7 and the MDR sub-line MCF-7/Dx. We demonstrate that these thiosulfinate derivatives show specificity towards MDR breast cancer cells and inhibit cell proliferation through the disruption of mitochondrial respiration, leading to the induction of apoptosis and cell cycle arrest.

Methods

Materials

IR spectra were recorded on an Agilent Cary 630 FTIR spectrometer (Agilent Technologies, Santa Clara, CA, USA). ^{1}H and ^{13}C NMR spectra were recorded on an Agilent 500 MHz NMR spectrometer in deuterated chloroform ($CDCl_3$) unless otherwise stated. Chemical shifts are quoted relative to residual chloroform (δ 7.26 for ^{1}H NMR and δ 77.36 for ^{13}C NMR) as an internal standard, and all chemical shifts (δ) are reported in parts per million (ppm). The coupling constants (*J*) are quoted in Hertz (Hz). The type of signal detected is indicated by the following abbreviations: s=singlet, d=doublet, t=triplet, q=quartet, tt=triplet of triplets, and m=multiplet. High-resolution mass spectrometry (HRMS) data were obtained using an Agilent 6510 Q-TOF LC/MS. DCM (dichloromethane), used under N_2 in the synthesis of asymmetric disulfides and the oxidation of thiosulfinates, was dried over molecular sieves. All other reagents and solvents were obtained from commercial suppliers and were used without further purification. All thiosulfinates were synthesized *via* a disulfide intermediate, except for allicin (**1b**), which was synthesized directly from diallyl disulfide purchased from Sigma-Aldrich (NSW, Australia). Thin-layer chromatography (TLC) was performed on Merck pre-coated silica gel plates (60 F_{254}), and spots were visualized by exposure to iodine vapor or short-wave UV light (l254 nm). Whenever required, column chromatography was performed using Scharlau silica gel 60 (230–400 mesh), with *n*-hexane and ethyl acetate used as eluents.

Synthesis of reaction catalysts

CsF-Celite

Celite 521 (3.20 g) was added to cesium fluoride (5.36 g, 32.0 mmol) dissolved in 80 mL of H_2O. The mixture was stirred for 30 min at RT, after which the H_2O was removed under reduced pressure. The resultant solid was then washed twice in CH_3CN, filtered, and dried in a desiccator at room temperature.

1-Chlorobenzotriazole

An 8%–12% NaOCl solution (commercial bleach) was added dropwise to a stirred solution of 50% acetic acid (32 mL) and benzotriazole (8 g, 67.2 mmol). Once the addition was complete, the reaction was stirred for 3 h. The product was then filtered and washed until the pH of the filtrate was neutral. The product was then dried under reduced pressure to obtain 1-chlorobenzotriazole (*m*-CBTA) as a white powder. The spectral data agree with values reported in the literature[41]. Yield: 94%; ^{1}H NMR δ (500 MHz, $CDCl_3$): 8.09 (1H, d, *J*=8.5 Hz), 7.61–7.47 (2H, m), 7.46–7.44 (1H, m) ppm; and ^{13}C NMR δ (500 MHz, $CDCl_3$): 144.46, 134.35, 129.55, 125.35, 120.99, 109.54 ppm.

General procedures for the synthesis of symmetrical disulfides

CsF-Celite (1.59 g) was stirred in 10 mL of acetonitrile, the appropriate thiol (5 mmol) was then added, and the solution was stirred for 5–48 h. The reaction progression was monitored by TLC. Once the reaction was complete, the mixture was filtered, and the filtrate evaporated under reduced pressure. The resultant disulfide was characterized by ^{1}H and ^{13}C and used in thiosulfinate synthesis without further purification.

1-(Ethyldisulfanyl)ethane (2a)[42]

Yield: 91%, as a yellow oil; ^{1}H NMR δ (500 MHz, $CDCl_3$): 2.70 (4H, q, *J*=7.5 Hz, SCH_2), 1.32 (6H, t, *J*=7.5 Hz, CH_3) ppm; ^{13}C NMR δ (500 MHz, $CDCl_3$): 33.27, 14.81 ppm.

1-(propyldisulfanyl)propane (3a)[42]

Yield: 97%, as a yellow oil; ^{1}H NMR δ (500 MHz, $CDCl_3$): 2.67 (4H, t, *J*=7.2 Hz, SCH_2), 1.71 (4H, sextet, *J*=7.2 Hz, SCH_2CH_2), 1.00 (6H, t, *J*=7.2 Hz, CH_3) ppm; ^{13}C NMR δ (500 MHz, $CDCl_3$): 41.54, 22.86, 13.47 ppm.

1-(Butyldisulfanyl)butane (4a)[42]

Yield: 92%, as a yellow oil; ^{1}H NMR δ (500 MHz, $CDCl_3$): 2.69

(4H, t, *J*=7.5 Hz, SCH_2), 1.65 (4H, quintet, *J*=7.5 Hz, SCH_2CH_2), 1.41 (4H, sextet, *J*=7.5 Hz, CH_2CH_3), 0.92 (6H, t, *J*=7.5 Hz, CH_3) ppm; ^{13}C NMR δ (500 MHz, $CDCl_3$): 39.25, 31.67, 22.01, 14.04 ppm.

1-(Hexyldisulfanyl)hexane (5a)[42]
Yield: 62%, as a yellow oil; ^{1}H NMR δ (500 MHz, $CDCl_3$): 2.68 (4H, t, *J*=6.8 Hz, SCH_2), 1.67 (4H, quintet, *J*=6.8 Hz, SCH_2CH_2), 1.41–1.26 (12H, m, $CH_2CH_2CH_2CH_3$), 0.89 (6H, t, *J*=6.8 Hz, CH_3), ppm; ^{13}C NMR δ (500 MHz, $CDCl_3$): 39.58, 31.79, 31.27, 29.54, 28.56, 14.37 ppm.

1-(4-Methylphenyldisulfanyl)-4-methylbenzene (6a)[43]
Yield: 90%, as a white solid; ^{1}H NMR δ (500 MHz, $CDCl_3$): 7.38 (4H, d, *J*=8.0 Hz, ArH-2), 7.10 (4H, d, *J*=8.0 Hz, ArH-3), 2.32 (6H, s, CH_3) ppm; ^{13}C NMR δ (500 MHz, $CDCl_3$): 137.80, 134.26, 130.14, 128.90, 21.41 ppm.

1-(4-Methoxyphenyldisulfanyl)-4-methoxylbenzene (13a)[43]
Yield: 91%, as a yellow oil; ^{1}H NMR δ (500 MHz, $CDCl_3$): 7.40 (4H, d, *J*=9.0 Hz, ArH-2), 6.83 (4H, d, *J*=9.0 Hz, ArH-3), 3.80 (6H, s, OCH_3) ppm; ^{13}C NMR δ (500 MHz, $CDCl_3$): 160.27, 133.02, 128.80, 114.96, 55.72 ppm.

1-(4-Tert-butylbenzyldisulfanyl)-4-tert-butylbenzene-1-methane (20a)[43]
Yield: 82%, as an orange solid; ^{1}H NMR δ (500 MHz, $CDCl_3$): 7.34 (2H, d, *J*=8.0 Hz, ArH-2), 7.17 (2H, d, *J*=8.0 Hz, ArH-3), 3.60 (2H, s, CH_2), 1.31 (9H, s, $C(CH_3)_3$) ppm; ^{13}C NMR δ (500 MHz, $CDCl_3$): 150.84, 134.57, 129.45, 125.76, 43.33, 34.90, 31.71 ppm.

General procedures for the synthesis of asymmetric disulfides
m-CBTA (0.61 g, 4.0 mmol) and benzotriazole (0.36 g, 3.0 mmol) were dissolved in dry DCM and stirred under a N_2 atmosphere at RT. The temperature was then reduced to -78 °C, and the appropriate thiol (R_1, 3.0 mmol, dissolved in dry DCM) was slowly added dropwise. The reaction mixture was then left to stir for 2 h. The second thiol (R_2, 3.2 mmol, dissolved in dry DCM) was then added slowly to the reaction. Once the addition was complete, the reaction mixture was allowed to warm to 0 °C and then stirred for a further 30 min. The reaction was then quenched with $Na_2S_2O_3$ (0.5 g in 15 mL H_2O) and stirred for a further 10 min at 0 °C. The organic fraction was then extracted with aqueous $NaHCO_3$ and then twice more with H_2O. The product was dried over anhydrous $MgSO_4$, and the solvent was removed under reduced pressure. The resultant disulfide was characterized by ^{1}H and ^{13}C and used in thiosulfinate synthesis without further purification.

1-(Ethyldisulfanyl)-4-methylbenzene (7a)[44]
Yield: 76%, as a yellow oil; ^{1}H NMR δ (500 MHz, $CDCl_3$): 7.43 (2H, d, *J*=8.5 Hz, ArH-2), 7.13 (2H, d, *J*=8.5 Hz, ArH-3), 2.74 (2H, q, *J*=7.0 Hz, CH_2CH_3), 2.33 (3H, s, $C_6H_4CH_3$), 1.31 (3H, t, *J*=7.0 Hz, CH_2CH_3) ppm; ^{13}C NMR δ (500 MHz, $CDCl_3$): 137.33, 134.57, 130.07, 128.69, 32.98, 21.37, 14.46 ppm.

1-(Propyldisulfanyl)-4-methylbenzene (8a)[40]
Yield: 89%, as a yellow oil; ^{1}H NMR δ (500 MHz, $CDCl_3$): 7.43 (2H, d, *J*=8.5 Hz, ArH-2), 7.13 (2H, d, *J*=8.5 Hz, ArH-3), 2.71 (2H, t, *J*=7.3 Hz, SCH_2), 2.33 (3H, s, $C_6H_4CH_3$), 1.70 (2H, sextet, *J*=7.3 Hz, CH_2CH_3), 0.96 (3H, t, *J*=7.3 Hz, CH_2CH_3) ppm; ^{13}C NMR δ (500 MHz, $CDCl_3$): 137.29, 134.55, 130.06, 128.64, 41.21, 22.48, 21.37, 13.44 ppm.

1-(Tert-butyldisulfanyl)-4-methylbenzene (9a)[45]
Yield: 92%, as a yellow oil; ^{1}H NMR δ (500 MHz, $CDCl_3$): 7.44 (2H, d, *J*=8.5 Hz, ArH-2), 7.10 (2H, d, *J*=8.5 Hz, ArH-3), 2.32 (3H, s, $C_6H_4CH_3$), 1.30 (9H, s, $C(CH_3)_3$) ppm; ^{13}C NMR δ (500 MHz, $CDCl_3$): 136.65, 135.71, 129.85, 127.76, 49.39, 30.22, 21.32 ppm.

1-(4-Tert-butylbenzyldisulfanyl)-4-methylbenzene (10a)
Yield: 54%, as a yellow oil; ^{1}H NMR δ (500 MHz, $CDCl_3$): 7.32 (2H, d, *J*=8.0 Hz, MeArH-2), 7.30 (2H, d, *J*=8.0 Hz, ArH-2), 7.21 (2H, d, *J*=8.0 Hz, ArH-3), 7.08 (2H, d, *J*=8.0 Hz, MeArH-3), 3.93 (2H, s, CH_2), 2.32 (3H, s, $C_6H_4CH_3$), 1.30 (9H, s, $C(CH_3)_3$) ppm; ^{13}C NMR δ (500 MHz, $CDCl_3$): 150.83, 137.32, 134.57, 134.09, 129.99, 129.45, 128.88, 125.75, 43.33, 34.89, 31.70, 21.37 ppm.

1-(4-Methylphenyldisulfanyl)-4-methoxybenzene (11a)[46]
Yield: 67%, as a yellow oil; ^{1}H NMR δ (500 MHz, $CDCl_3$): 7.41 (2H, d, *J*=8.5 Hz, MeOArH-2), 7.38 (2H, d, *J*=8.5 Hz, ArH-2), 7.11 (2H, d, *J*=8.5 Hz, ArH-3), 6.83 (2H, d, *J*=8.5 Hz, MeOArH-3), 3.79 (3H, s, OCH_3), 2.33 (3H, s, $C_6H_4CH_3$) ppm; ^{13}C NMR δ (500 MHz, $CDCl_3$): 160.14, 137.96, 134.41, 132.30, 130.12, 128.88, 128.66, 114.00, 55.71, 21.43 ppm.

1-(Ethyldisulfanyl)-4-methoxybenzene (14a)
Yield: 76%, as a yellow oil; ^{1}H NMR δ (500 MHz, $CDCl_3$): 7.48 (2H, d, *J*=9.0 Hz, ArH-2), 6.86 (2H, d, *J*=9.0 Hz, ArH-3), 3.80 (3H, s, OCH_3), 2.74 (2H, q, *J*=7.5 Hz, SCH_2), 1.31 (3H, t, *J*=7.5 Hz, CH_2CH_3) ppm; ^{13}C NMR δ (500 MHz, $CDCl_3$): 159.84, 131.99, 128.90, 114.97, 55.74, 32.91, 14.42 ppm.

1-(Butyldisulfanyl)-4-methoxybenzene (15a)[47]
Yield: 69%, as a yellow oil; ^{1}H NMR δ (500 MHz, $CDCl_3$): 7.48 (2H, d, *J*=9.0 Hz, ArH-2), 6.86 (2H, d, *J*=9.0 Hz, ArH-3), 3.81 (3H, s, OCH_3), 2.73 (2H, t, *J*=7.5 Hz, SCH_2), 1.65 (2H, quintet, *J*=7.5 Hz, SCH_2CH_2), 1.38 (2H, sextet, *J*=7.5 Hz, CH_2CH_3), 0.89 (3H, t, *J*=7.5 Hz, CH_2CH_3) ppm; ^{13}C NMR δ (500 MHz, $CDCl_3$): 159.83, 131.97, 128.90, 114.97, 55.75, 38.87, 31.13, 21.97, 13.98 ppm.

1-(Tert-butyldisulfanyl)-4-methoxybenzene (16a)[45]
Yield: 84%, as a yellow oil; ^{1}H NMR δ (500 MHz, $CDCl_3$): 7.49 (2H, d, *J*=9.0 Hz, ArH-2), 6.84 (2H, d, *J*=9.0 Hz, ArH-3), 3.79 (3H, s, OCH_3), 1.29 (9H, s, $C(CH_3)_3$) ppm; ^{13}C NMR δ (500 MHz, $CDCl_3$): 159.27, 130.63, 130.11, 114.77, 55.71, 49.28, 30.25 ppm.

1-(Hexyldisulfanyl)-4-methoxybenzene (17a)[46]
Yield: 85%, as a yellow oil; ^{1}H NMR δ (500 MHz, $CDCl_3$): 7.48

(2H, d, *J*=9.0 Hz, ArH-2), 6.86 (2H, d, *J*=9.0 Hz, ArH-3), 3.81 (3H, s, OCH_3), 2.73 (2H, t, *J*=7.5 Hz, SCH_2), 1.66 (2H, quintet, *J*=7.5 Hz, SCH_2CH_2), 1.38-1.23 (6H, m, $CH_2CH_2CH_2CH_3$), 0.87 (3H, t, *J*=7.5 Hz, CH_3) ppm; ^{13}C NMR δ (500 MHz, $CDCl_3$): 159.83, 132.00, 128.93, 114.96, 55.75, 39.25, 31.72, 29.02, 28.50, 22.85, 14.36 ppm.

1-(Cyclohexyldisulfanyl)-4-methoxybenzene (18a)[47]

Yield: 89%, as a yellow oil; ^{1}H NMR δ (500 MHz, $CDCl_3$): 7.47 (2H, d, *J*=9.0 Hz, ArH-2), 6.86 (2H, d, *J*=9.0 Hz, ArH-3), 3.80 (3H, s, OCH_3), 2.80 (1H, tt, *J*=10.5, 3.7 Hz, H-1), 2.03-2.00 (2H, m, H-6), 1.78–1.75 (2H, m, H-2), 1.61–1.58 (1H, m, H-4_a), 1.39-1.20 (5H, m, H-3, H-5 and H-4_b) ppm; ^{13}C NMR δ (500 MHz, $CDCl_3$): 159.46, 131.03, 129.69, 114.85, 55.70, 49.99, 32.90, 26.32, 25.97 ppm.

1-(4-Tert-butylbenzyldisulfanyl)-4-methoxybenzene (19a)

Yield: 64%, as a yellow oil; ^{1}H NMR δ (500 MHz, $CDCl_3$): 7.34 (2H, d, *J*=9.0 Hz, MeOArH-2), 7.30 (2H, d, *J*=9.0 Hz, ArH-2), 7.21 (2H, d, *J*=9.0 Hz, ArH-3), 6.80 (2H, d, *J*=9.0 Hz, MeOArH-3), 3.93 (2H, s, CH_2), 3.80 (3H, s, CH_3), 1.31 (9H, s, $C(CH_3)_3$) ppm; ^{13}C NMR δ (500 MHz, $CDCl_3$): 159.81, 150.78, 134.06, 132.19, 129.44, 128.47, 125.79, 114.86, 55.70, 43.46, 34.87, 31.70 ppm.

4-(Butyldisulfanyl)phenol (21a)

Yield: 41%, as a yellow oil; ^{1}H NMR δ (500 MHz, $CDCl_3$): 7.43 (2H, d, *J*=8.5 Hz, ArH-2), 6.80 (2H, d, *J*=8.5 Hz, ArH-3), 2.73 (2H, t, *J*=7.5 Hz, SCH_2), 1.73 (2H, quintet, *J*=7.5 Hz, SCH_2CH_2), 1.41 (2H, sextet, *J*=7.5 Hz, CH_2CH_3), 0.88 (3H, t, *J*=7.5 Hz, CH_3) ppm; ^{13}C NMR δ (500 MHz, $CDCl_3$): 155.94, 132.17, 117.49, 116.46, 39.23, 31.65, 21.00, 14.03 ppm.

4-(hexyldisulfanyl)phenol (22a)

Yield: 35%, as a yellow oil; ^{1}H NMR δ (500 MHz, $CDCl_3$): 7.43 (2H, d, *J*=8.5 Hz, ArH-2), 6.81 (2H, d, *J*=8.5 Hz, ArH-3), 2.73 (2H, t, *J*=7.5 Hz, SCH_2), 1.74 (2H, quintet, *J*=7.5 Hz, SCH_2CH_2), 1.44-1.23 (6H, m, $CH_2CH_2CH_2CH_3$), 0.87 (3H, t, *J*=7.5 Hz, CH_3) ppm; ^{13}C NMR δ (500 MHz, $CDCl_3$): 155.90, 132.15, 117.46, 116.43, 39.24, 31.70, 29.13, 28.54, 22.85, 14.35 ppm.

General procedures for the synthesis of symmetric and asymmetric thiosulfinates

The selected disulfide (3.0 mmol) was dissolved in dry DCM (5 mL) under a N_2 atmosphere at -78 °C. *m*-CPBA (0.52 g, 3.0 mmol), dissolved in dry DCM (5 mL), was then slowly added dropwise. Once the addition was complete, the reaction was left to stir for 3 h, slowly warming to 0 °C. The reaction was quenched with saturated $NaHCO_3$, and the resulting aqueous solution was extracted 3 times with DCM. The combined organic fractions were then dried over anhydrous $MgSO_4$ and evaporated under reduced pressure. The crude product was then purified by silica gel flash column chromatography (*n*-hexane/ethyl acetate). After purification, all thiosulfinates were stored at -80 °C until required. All stock solutions were prepared in DMSO and stored at -20 °C.

Allicin, S-allyl prop-2-ene-1-sulfinothioate (1b)[39]

Yield: 23%, as a yellow oil; IR υ_{max} cm^{-1}: 1060 (S=O); ^{1}H NMR δ (500 MHz, D_2O): 6.05–5.94 (m, 2H, SCH_2CH), 5.53–4.79 (m, 4H, $CH=CH_2$), 4.05–3.82 (m, 4H, SCH_2) ppm; ^{13}C NMR δ (500 MHz, D_2O): 136.01, 128.07, 127.87, 121.00, 61.07, 38.47 ppm; HRMS *m/z*: calcd. for $C_6H_{10}OS_2$ $(M+H)^+$: 163.0246; found: 163.0245.

S-ethyl ethanesulfinothioate (2b)[39]

Yield: 46%, as a yellow oil; IR υ_{max} cm^{-1}: 1074 (S=O); ^{1}H NMR δ (500 MHz, $CDCl_3$): 3.18–3.11 (4H, m, SCH_2), 1.46 (3H, t, *J*=7.5 Hz, SCH_2CH_3), 1.40 (3H, t, *J*=7.5 Hz, $S=OCH_2CH_3$) ppm; ^{13}C NMR δ (500 MHz, $CDCl_3$): 50.26, 27.38, 16.58, 8.12 ppm; HRMS *m/z*: calcd. for $C_4H_{10}OS_2$ $(M+H)^+$: 139.0246; found: 139.0243.

S-propyl propane-1-sulfinothioate (3b)[39]

Yield: 51%, as a yellow oil; IR υ_{max} cm^{-1}: 1076 (S=O); ^{1}H NMR δ (500 MHz, D_2O): 3.26-3.19 (4H, m, SCH_2), 1.86-1.80 (4H, m, SCH_2CH_2), 1.07 (3H, t, *J*=7.5 Hz, ($SCH_2CH_2CH_3$), 1.02 (3H, t, *J*=7.5 Hz, $S=OCH_2CH_2CH_3$) ppm; ^{13}C NMR δ (500 MHz, D_2O): 59.65, 38.20, 26.59, 19.70, 15.07, 15.00 ppm; HRMS *m/z*: calcd. for $C_6H_{14}OS_2$ $(M+H)^+$: 167.0559; found: 167.0562.

S-butyl butane-1-sulfinothioate (4b)[39]

Yield: 57%, as a yellow oil; IR υ_{max} cm^{-1}: 1081 (S=O); ^{1}H NMR δ (500 MHz, $CDCl_3$): 3.15–3.10 (4H, m, SCH_2), 1.82–1.75 (4H, m, SCH_2CH_2), 1.50–1.43 (4H, m, CH_2CH_3), 0.98–0.93 (6H, m, CH_3) ppm; ^{13}C NMR δ (500 MHz, $CDCl_3$): 56.33, 33.22, 32.95, 25.81, 22.21, 22.08, 14.01, 13.86 ppm; HRMS *m/z*: calcd. for $C_8H_{18}OS_2$ $(M+H)^+$: 195.0872; found: 195.0873.

S-hexyl hexane-1-sulfinothioate (5b)[17]

Yield: 48%, as a yellow oil; IR υ_{max} cm^{-1}: 1079 (S=O); ^{1}H NMR δ (500 MHz, $CDCl_3$): 3.16-3.08 (4H, m, SCH_2), 1.84–1.77 (4H, m, SCH_2CH_2), 1.46–1.41 (4H, m, $S(CH_2)_2CH_2$), 1.35–1.29 (8H, m, $CH_2CH_2CH_3$), 0.91–0.88 (6H, m, CH_3) ppm; ^{13}C NMR δ (500 MHz, $CDCl_3$): 56.62, 33.26, 31.67, 31.57, 31.17, 28.63, 28.61, 23.78, 22.83, 22.73, 14.34, 14.30 ppm; HRMS *m/z*: calcd. for $C_{12}H_{26}OS_2$ $(M+H)^+$: 251.1498; found: 251.1496.

S-4-tolyl 4-methylbenzenesulfinothioate (6b)[48]

Yield: 24%, as a white solid; IR υ_{max} cm^{-1}: 1075 (S=O); ^{1}H NMR δ (500 MHz, $CDCl_3$): 7.46 (2H, d, *J*=8.0 Hz, ArH-2), 7.24 (2H, d, *J*=8.0 Hz, ArH-2′), 7.21 (2H, d, *J*=8.0 Hz, ArH-3), 7.14 (2H, d, *J*=8.0 Hz, ArH-3′), 2.42 (3H, s, CH_3′), 2.38 (3H, s, CH_3-1) ppm; ^{13}C NMR δ (500 MHz, $CDCl_3$): 144.91, 142.38, 140.84, 136.85, 130.54, 129.71, 127.96, 124.96, 22.01, 21.83 ppm; HRMS *m/z*: calcd. for $C_{14}H_{14}OS_2$ $(M+H)^+$: 263.0559; found: 263.0557.

S-4-tolyl ethanesulfinothioate (7b)

Yield: 39%, as a yellow oil; IR υ_{max} cm^{-1}: 1079 (S=O); ^{1}H NMR δ (500 MHz, $CDCl_3$): 7.49 (2H, d, *J*=7.5 Hz, ArH-2), 7.22 (2H, d, *J*=7.5 Hz, ArH-3), 3.10 (2H, q, *J*=7.5 Hz, $S=OCH_2$), 2.38 (3H, s, $C_6H_4CH_3$), 1.43 (3H, t, *J*=7.5 Hz, CH_2CH_3) ppm; ^{13}C NMR δ (500 MHz, $CDCl_3$): 141.06, 135.73, 130.62, 125.58, 50.22, 21.70, 8.24 ppm; HRMS *m/z*: calcd. for $C_9H_{12}OS_2$ $(M+H)^+$: 201.0402; found: 201.0404.

***S*-4-tolyl propane-1-sulfinothioate (8b)**[40]

Yield: 41%, as a yellow oil; IR v_{max} cm^{-1}: 1080 (S=O); ^1H NMR δ (500 MHz, $CDCl_3$): 7.50 (2H, d, *J*=8.0 Hz, ArH-2), 7.23 (2H, d, *J*=8.0 Hz, ArH-3), 3.08 (2H, m, S=OCH_2), 2.39 (3H, s, $C_6H_4CH_3$), 1.89 (2H, m, CH_2CH_3), 1.10 (3H, t, *J*=7.5 Hz, CH_2CH_3) ppm; ^{13}C NMR δ (500 MHz, $CDCl_3$): 141.04, 135.66, 130.59, 125.83, 58.16, 21.68, 17.59, 13.58 ppm; HRMS *m/z*: calcd. for $C_{10}H_{14}OS_2$ $(M+H)^+$: 215.0559; found: 215.0558.

***S*-4-tolyl 2-methylpropane-2-sulfinothioate (9b)**[49]

Yield: 17%, as a white solid; IR v_{max} cm^{-1}: 1078 (S=O); ^1H NMR δ (500 MHz, $CDCl_3$): 7.52 (2H, d, *J*=8.0 Hz, ArH-2), 7.20 (2H, d, *J*=8.0 Hz, ArH-3), 2.38 (3H, s, $C_6H_4CH_3$), 1.46 (9H, s, $C(CH_3)_3$) ppm; ^{13}C NMR δ (500 MHz, $CDCl_3$): 140.52, 135.59, 130.60, 126.51, 60.47, 24.50, 21.63 ppm; HRMS *m/z*: calcd. for $C_{11}H_{16}OS_2$ $(M+H)^+$: 229.0715; found: 229.0715.

***S*-4-tolyl (4-tert-butylphenyl)methanesulfinothioate (10b)**

Yield: 33%, as a white solid; IR v_{max} cm^{-1}: 1078 (S=O); ^1H NMR δ (500 MHz, $CDCl_3$): 7.44 (2H, d, *J*=8.5 Hz, MeArH-2), 7.41 (2H, d, *J*=8.5 Hz, ArH-2), 7.30 (2H, d, *J*=8.5 Hz, ArH-3), 7.19 (2H, d, *J*=8.5 Hz, MeArH-3), 4.37 (1H, d, *J*=13.0 Hz, CH_a), 4.25 (1H, d, *J*=13.0 Hz, CH_b), 2.37 (3H, s, $C_6H_4CH_3$), 1.33 (9H, s, $C(CH_3)_3$) ppm; ^{13}C NMR δ (500 MHz, $CDCl_3$): 152.09, 141.02, 135.80, 130.59, 130.44, 127.38, 126.21, 125.80, 62.50, 35.03, 31.62, 21.69 ppm; HRMS *m/z*: calcd. for $C_{18}H_{22}OS_2$ $(M+H)^+$: 319.1185; found: 319.1187.

***S*-4-methoxyphenyl 4-methylbenzenesulfinothioate (11b)**[48]

Yield: 20%, as a white solid; IR v_{max} cm^{-1}: 1075 (S=O); ^1H NMR δ (500 MHz, $CDCl_3$): 7.53 (2H, d, *J*=8.0 Hz, MeOArH-2), 7.43 (2H, d, *J*=8.0 Hz, ArH-2), 7.29 (2H, d, *J*=8.0 Hz, ArH-3), 6.89 (2H, d, *J*=8.0 Hz, MeOArH-3), 3.84 (3H, s, OCH_3) 2.42 (3H, s, $C_6H_4CH_3$) ppm; ^{13}C NMR δ (500 MHz, $CDCl_3$): 161.90, 142.48, 135.80, 129.94, 129.74, 124.67, 120.32, 115.18, 55.80, 21.87 ppm; HRMS *m/z*: calcd. for $C_{14}H_{14}O_2S_2$ $(M+H)^+$: 279.0508; found: 279.0504.

***S*-4-tolyl 4-methoxybenzenesulfinothioate (12b)**[48]

Yield: 20%, as a white solid; IR v_{max} cm^{-1}: 1075 (S=O); ^1H NMR δ (500 MHz, $CDCl_3$): 7.60 (2H, d, *J*=8.5 Hz, MeOArH-2), 7.43 (2H, d, *J*=8.5 Hz, ArH-2), 7.19 (2H, d, *J*=8.5 Hz, ArH-3), 6.99 (2H, d, *J*=8.5 Hz, MeOArH-3), 3.87 (3H, s, OCH_3) 2.38 (3H, s, $C_6H_4CH_3$) ppm; ^{13}C NMR δ (500 MHz, $CDCl_3$): 162.60, 141.08, 137.85, 130.42, 127.97, 126.53, 126.50, 114.76, 55.94, 21.73 ppm; HRMS *m/z*: calcd. for $C_{14}H_{14}O_2S_2$ $(M+H)^+$: 279.0508; found: 279.0504.

***S*-4-methoxyphenyl 4-methoxybenzenesulfinothioate (13b)**[50]

Yield: 74%, as a yellow solid; IR v_{max} cm^{-1}: 1073 (S=O); ^1H NMR δ (500 MHz, $CDCl_3$): 7.56 (2H, d, *J*=8.5 Hz, ArH-2), 7.42 (2H, d, *J*=8.5 Hz, ArH-2′), 6.98 (2H, d, *J*=8.5 Hz, ArH-3′), 6.89 (2H, d, *J*=8.5 Hz, ArH-3), 3.86 (3H, s, OCH_3-2) 3.84 (3H, s, OCH_3-1) ppm; ^{13}C NMR δ (500 MHz, $CDCl_3$): 162.56, 162.01, 137.88, 135.55, 126.51, 120.31, 115.15, 114.71, 55.94, 55.80 ppm; HRMS *m/z*: calcd. for $C_{14}H_{14}O_3S_2$ $(M+H)^+$: 295.0457; found: 295.0457.

***S*-4-methoxyphenyl ethanesulfinothioate (14b)**

Yield: 48%, as a yellow oil; IR v_{max} cm^{-1}: 1076 (S=O); ^1H NMR δ (500 MHz, $CDCl_3$): 7.53 (2H, d, *J*=9.0 Hz, ArH-2), 6.94 (2H, d, *J*=9.0 Hz, ArH-3), 3.84 (3H, s, OCH_3), 3.07 (2H, q, *J*=7.5 Hz, CH_2CH_3), 1.42 (3H, t, *J*=7.5 Hz, CH_2CH_3) ppm; ^{13}C NMR δ (500 MHz, $CDCl_3$): 161.95, 137.76, 119.28, 115.42, 55.80, 49.98, 8.22 ppm; HRMS *m/z:* calcd. for $C_9H_{12}O_2S_2$ $(M+H)^+$: 217.0351; found: 217.0350.

***S*-4-methoxyphenyl butane-1-sulfinothioate (15b)**

Yield: 39%, as a yellow oil; IR v_{max} cm^{-1}: 1080 (S=O); ^1H NMR δ (500 MHz, $CDCl_3$): 7.53 (2H, d, *J*=9.0 Hz, ArH-2), 6.94 (2H, d, *J*=9.0 Hz, ArH-3), 3.84 (3H, s, OCH_3), 3.06 (2H, t, *J*=7.5 Hz, SCH_2), 1.82 (2H, m, SCH_2CH_2), 1.45 (2H, m, CH_2CH_3), 0.98 (3H, t, *J*=7.5 Hz, CH_2CH_3) ppm; ^{13}C NMR δ (500 MHz, $CDCl_3$): 161.94, 137.72, 119.57, 115.41, 55.94, 55.80, 25.84, 22.29, 14.05 ppm; HRMS *m/z*: calcd. for $C_{11}H_{16}O_2S_2$ $(M+H)^+$: 245.0664; found: 245.0665.

***S*-4-methoxyphenyl 2-methylpropane-2-sulfinothioate (16b)**

Yield: 27%, as a white solid; IR v_{max} cm^{-1}: 1072 (S=O); ^1H NMR δ (500 MHz, $CDCl_3$): 7.55 (2H, d, *J*=8.5 Hz, ArH-2), 6.92 (2H, d, *J*=8.5 Hz, ArH-3), 3.83 (3H, s, OCH_3), 1.45 (9H, s, $C(CH_3)_3$) ppm; ^{13}C NMR δ (500 MHz, $CDCl_3$): 161.62, 137.63, 120.24, 115.44, 60.27, 55.78, 24.50 ppm; HRMS *m/z*: calcd. for $C_{11}H_{16}O_2S_2$ $(M+H)^+$: 245.0664; found: 245.0660.

***S*-4-methoxyphenyl hexane-1-sulfinothioate (17b)**

Yield: 51%, as a yellow oil; IR v_{max} cm^{-1}: 1078 (S=O); ^1H NMR δ (500 MHz, $CDCl_3$): 7.53 (2H, d, *J*=9.0 Hz, ArH-2), 6.94 (2H, d, *J*=9.0 Hz, ArH-3), 3.84 (3H, s, OCH_3), 3.05 (2H, t, *J*=7.5 Hz, SCH_2), 1.84-1.81 (2H, m, SCH_2CH_2), 1.46-1.31 (6H, m, $CH_2CH_2CH_2CH_3$), 0.90 (3H, t, *J*=7.5 Hz, CH_3) ppm; ^{13}C NMR δ (500 MHz, $CDCl_3$): 161.94, 137.72, 119.59, 115.41, 56.21, 55.80, 31.69, 28.70, 23.80, 22.73, 14.31 ppm; HRMS *m/z*: calcd. for $C_{13}H_{20}O_2S_2$ $(M+H)^+$: 273.0977; found: 273.0974.

***S*-4-methoxyphenyl cyclohexanesulfinothioate (18b)**

Yield: 38%, as a white solid; IR v_{max} cm^{-1}: 1077 (S=O); ^1H NMR δ (500 MHz, $CDCl_3$): 7.52 (2H, d, *J*=8.5 Hz, ArH-2), 6.92 (2H, d, *J*=8.5 Hz, ArH-3), 3.82 (3H, s, OCH_3), 2.99 (1H, tt, *J*=11.5, 3.9 Hz, H-1), 2.17–2.14 (2H, m, H-6), 1.94–1.88 (2H, m, H-2), 1.71–1.50 (3H, m, H-3 and H-4_a), 1.41–1.25 (3H, m, H-5 and H-4_b) ppm; ^{13}C NMR δ (500 MHz, $CDCl_3$): 161.71, 137.56, 119.86, 115.35, 63.74, 55.73, 27.50, 26.52, 25.86, 25.77, 25.69 ppm; HRMS *m/z*: calcd. for $C_{13}H_{18}O_2S_2$ $(M+H)^+$: 271.0821; found: 271.0824.

***S*-4-methoxyphenyl (4-tert-butylphenyl)methanesulfinothioate (19b)**

Yield: 29%, as a yellow oil; IR v_{max} cm^{-1}: 1074 (S=O); ^1H NMR δ (500 MHz, $CDCl_3$): 7.48 (2H, d, *J*=8.5 Hz, MeOArH-2), 7.41 (2H, d, *J*=8.5 Hz, ArH-2), 7.30 (2H, d, *J*=8.5 Hz, ArH-3), 6.91 (2H, d, *J*=8.5 Hz, MeOArH-3), 4.34, (1H, d, *J*=13.0 Hz, CH_a), 4.22 (1H, d, *J*=13.0 Hz, CH_b), 3.82 (3H, s, OCH_3), 1.33 (9H, s, $C(CH_3)_3$) ppm; ^{13}C NMR δ (500 MHz, $CDCl_3$): 161.92, 152.06, 137.84, 130.42, 127.42, 126.21, 119.54, 115.39, 62.35, 55.79, 35.03,

31.62 ppm; HRMS *m/z*: calcd. for $C_{18}H_{22}O_2S_2$ $(M+H)^+$: 335.1134; found: 335.1137.

***S*-4-tert-butylphenyl (4-tert-butylphenyl)methanesulfinothioate (20b)**

Yield: 67%, as a white solid; IR υ_{max} cm^{-1}: 1067 (S=O); ^1H NMR δ (500 MHz, $CDCl_3$): 7.38 (2H, d, *J*=8.5 Hz, ArH-2), 7.33 (2H, d, *J*=8.5 Hz, ArH-2′), 7.25 (2H, d, *J*=8.5 Hz, ArH-3′), 7.24 (2H, d, *J*=8.5 Hz, ArH-3), 4.29–4.25 (4H, m, CH_2), 1.31 (9H, s, $C(CH_3)_3$-1), 1.30 (9H, s, $C(CH_3)_3$-2) ppm; ^{13}C NMR δ (500 MHz, $CDCl_3$): 152.04, 151.08, 133.82, 130.387, 129.17, 127.31, 126.11, 126.06, 62.15, 36.14, 34.97, 34.88, 31.61, 31.59 ppm; HRMS *m/z*: calcd. for $C_{22}H_{30}OS_2$ $(M+H)^+$: 375.1811; found: 375.1811.

***S*-4-hydroxyphenyl butane-1-sulfinothioate (21b)**

Yield: 17%, as a yellow oil; IR υ_{max} cm^{-1}: 1036 (S=O); ^1H NMR δ (500 MHz, $CDCl_3$): 7.40 (2H, d, *J*=8.5 Hz, ArH-2), 6.75 (2H, d, *J*=8.5 Hz, ArH-3), 3.11 (2H, t, *J*=7.5 Hz, SCH_2), 1.84 (2H, dq, *J*=7.5, 3.5 Hz, SCH_2CH_2), 1.51 (2H, ds, *J*=7.5, 3.5 Hz, CH_2CH_3), 0.99 (3H, t, *J*=7.5 Hz, CH_3) ppm; ^{13}C NMR δ (500 MHz, $CDCl_3$): 159.46, 138.09, 117.53, 117.39, 55.39, 25.84, 22.25, 14.03 ppm; HRMS *m/z*: calcd. for $C_{10}H_{14}O_2S_2$ $(M+H)^+$: 231.0508; found: 231.0507.

***S*-4-hydroxyphenyl hexane-1-sulfinothioate (22b)**

Yield: 12%, as a yellow oil; IR υ_{max} cm^{-1}: 1038 (S=O); ^1H NMR δ (500 MHz, $CDCl_3$): 7.40 (2H, d, *J*=8.5 Hz, ArH-2), 6.74 (2H, d, *J*=8.5 Hz, ArH-3), 3.10 (2H, t, *J*=7.5 Hz, SCH_2), 1.85 (2H, quintet, *J*=7.5 Hz, SCH_2CH_2), 1.49–1.46 (2H, m, $SCH_2CH_2CH_2$), 1.36–1.32 (4H, m, $CH_2CH_2CH_3$), 0.91 (3H, t, *J*=7.5 Hz, CH_3) ppm; ^{13}C NMR δ (500 MHz, $CDCl_3$): 159.37, 138.09, 117.60, 117.37, 55.66, 31.65, 28.65, 23.80, 22.72, 14.30 ppm; HRMS *m/z*: calcd. for $C_{12}H_{18}O_2S_2$ $(M+H)^+$: 259.0821; found: 259.0824.

Cell culture

The drug-sensitive human breast adenocarcinoma cell line MCF-7 and its drug-resistant sub-line, MCF-7/Dx (designated Dx for simplicity), were used in this study. Cells were grown in RPMI-1640 media (Sigma-Aldrich, NSW, Australia) supplemented with 10% heat-inactivated fetal bovine serum (Invitrogen, Life Technologies, Victoria, Australia) and maintained at 37 °C and 5% CO_2. Dx cells were initially developed from MCF-7 cells by incremental exposure to doxorubicin[51]. To maintain the MDR phenotype, Dx cells were cultured in the presence of 1 μg/mL doxorubicin; however, during experiments, cells were cultured in the absence of doxorubicin. Cells were routinely tested for mycoplasma contamination.

Cell antiproliferative activity assay

The anticancer activity of the synthesized compounds was determined using the MTS assay. Cells were seeded in 96-well plates (5×10^3 cells per well) and, once adherent, were cultured for 72 h in the presence of selected thiosulfinates at the indicated concentrations. Due to the short half-life of allicin, cells were treated with fresh media supplemented with the appropriate concentration of allicin every 24 h. Control cells were incubated with DMSO at 0.1% (*v/v*). Cell viability was determined using the CellTiter 96® AQueous One Solution Cell Proliferation Assay (Promega, USA) according to the manufacturer's recommendation. Briefly, following 72 h of treatment, 20 μL of the MTS reagent 3-(4,5-dimethyl-2-yl)-5-(3-carboxymethoxyphenyl)-2-(4-sulfophenyl)-2*H*-tetrazolium was added to each well and then incubated for 2 h in the dark at 37 °C. Absorbance values were then obtained at 490 nm (infinite M1000Pro, Tecan), and blank-subtracted absorbance values were normalized to the vehicle control, which was arbitrarily assigned as 100%. IC_{50} values were defined as the drug concentration that prevented cell growth of more than 50% relative to the vehicle control and were determined using non-linear regression analysis with Prism 7.0 (GraphPad Software, CA, USA).

Cell cycle analysis

Flow cytometric analysis was performed to calculate the distribution of the cell population through cell cycle phases. Cells were seeded in 6-well plates (5×10^5 cells per well) and, once adherent, were cultured for 24 h in the presence of selected thiosulfinates at the indicated concentrations. Colchicine was used as a positive control at 1 μmol/L (Supplementary material), and control cells were incubated with DMSO at 0.1% (*v/v*). After incubation, the cells were harvested, washed twice with PBS, and fixed with 70% ice-cold ethanol for at least 24 h. The fixed cells were then washed twice with PBS, resuspended in fresh PBS containing 0.1 mg/mL RNase A, 20 μg/mL propidium iodide (PI) and 0.1% (*v/v*) Triton X-100, and then incubated in the dark at 37 °C for 30 min. After incubation, the cells were analyzed by flow cytometry (LSRFortessa X-20, BD Biosciences), with 1×10^4 events per sample acquired. Cell cycle distribution was calculated using FlowJo version 10.1 (Tree Star, Inc, Australia).

Apoptosis studies

The extent of apoptosis was quantitatively measured using the Annexin V binding assay according to the manufacturer's recommendation (BD Biosciences, Sydney, NSW, Australia). Cells were seeded in 6-well plates (5×10^5 cells per well) and, once adherent, were cultured for 24 h in the presence of selected thiosulfinates at the indicated concentrations. Control cells were incubated with DMSO at 0.1% (*v/v*). After the incubation period, cells were harvested and washed twice with PBS and then resuspended in 1×binding buffer (1×10^6 cells/mL). Next, 5 μL of Annexin V and 5 μL of PI (BD Pharmingen, North Ryde, NSW, Australia) were added to a 100-μL aliquot of the cell suspension, which was then vortexed and incubated at RT in the dark for 15 min. Subsequently, 200 μL of 1×binding buffer was added to the mixture, and the cells were analyzed immediately by flow cytometry (LSRFortessa X-20, BD Biosciences), with 1×10^4 events per sample acquired. The percentages of viable (Annexin V^-/PI^-), early apoptotic (Annexin V^+/PI^-), late apoptotic (Annexin V^+/PI^+), and necrotic (Annexin V^-/PI^+) cells were calculated using FlowJo version 10.1 (Tree

Star, Inc).

Measurement of mitochondrial function

Mitochondrial function was measured by determining the oxygen consumption rate (OCR) of cells with a Seahorse XF24 extracellular flux analyzer (Seahorse Bioscience, MA, USA) according to the manufacturer's protocol. Cells were seeded in 24-well XF cell culture microplates (2×10^4 cells per well) and, once adherent, were cultured with selected thiosulfinates for 24 h at 37 °C and 5% CO_2. Prior to analysis, cells were washed, and the supernatant was replaced with buffered XF Base Medium supplemented with 2 mmol/L *L*-glutamine, 10 mmol/L glucose and 2 mmol/L sodium pyruvate at pH=7.4. The cells were incubated at 37 °C without CO_2 for an hour, and then, the OCR was measured utilizing an XF Cell Mito Stress Test Kit (Seahorse Bioscience, MA, USA). Oligomycin (final concentration 1 μmol/L), carbonylcyanide *m*-chlorophenylhydrazone (FCCP-final concentration 0.5 μmol/L), and rotenone/antimycin A (final concentration 0.5 μmol/L) were added to the sensor cartridge, and the OCR was measured using the standard cycling program.

Cell imaging

Cells were treated with thiosulfinates to examine effects on cellular morphology. Cells were seeded in 6-well plates (7×10^5 cells per well) and, once adherent, were cultured for 24 h in the presence of selected thiosulfinates at the indicated concentrations. Control cells were incubated with DMSO at 0.1% (*v/v*). After the incubation period, images were captured on a digital camera (INFINITY 1, Lumenera, Ottawa).

Trypan blue exclusion assay

Cells were harvested and stained with Trypan blue, and viable cells were counted on a hemocytometer. Cell mortality was expressed as a percentage of viable cells relative to the vehicle control. The vehicle control DMSO concentration did not exceed 0.1% (*v/v*).

Calculation of drug-likeness properties and toxicity prediction

Toxicity risk parameters and drug-likeness properties were calculated using OSIRIS Property Explorer. OSIRIS analyzes molecules with respect to Lipinski's rule of five, generating both a drug-likeness score and an overall drug score in addition to identifying any toxicity risks[52, 53]. To comply with Lipinski's rule of five, compounds must have a molecular weight of less than 500 g/mol, Log*P*≤5, hydrogen bond donors ≤5, hydrogen bond acceptors ≤10, a solubility score between -5 and 1, and a polar surface area less than 120 Å^2.

Statistical analysis

For *in vitro* assays, data were analyzed using one-way analysis of variance (ANOVA) followed by Tukey's *post hoc* analysis. $P<0.05$ were accepted as being statistically significant. All statistical analyses were performed using GraphPad Prism version 7.0 (GraphPad Software, CA, USA). The results are expressed as the mean±SEM unless otherwise noted.

Results

Chemistry

The symmetric disulfides **2a–6a**, **13a** and **20a** were synthesized via oxidative coupling (Scheme 1, Eq 1) using CsF-Celite as a solid base[54]. Synthesis of the short chain disulfides, **2a–4a**, was carried out at room temperature, after which any remaining starting materials were removed under reduced pressure to generate the pure disulfides at good yields (>90%). For disulfides **5a–6a**, **13a** and **20a,** it was found that at room temperature, only trace amounts of the product were formed after a 48-h period. These compounds were instead synthesized under reflux, which improved yields.

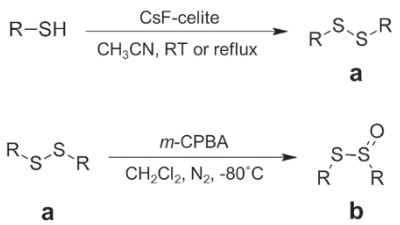

Compound	R	Compound	R
1	CH_2CHCH_2	**5**	$CH_3(CH_2)_4CH_2$
2	CH_3CH_2	**6**	4-CH_3Ph
3	$CH_3CH_2CH_2$	**13**	4-OCH_3Ph
4	$CH_3(CH_2)_2CH_2$	**20**	4-(*t*-Bu)$PhCH_2$

Scheme 1. Synthetic methods for the preparation of symmetric thiosulfinates **1b–6b**, **13b** and **20b.**

The asymmetric disulfides **7a–11a**, **14a–19a,** and **21a–22a** were synthesized by nucleophilic substitution (Scheme 2, Eq 3) via a sulfenyl chloride intermediate[46], and all symmetric and asymmetric disulfides were used in the next synthesis step without any further purification. Symmetric and asymmetric disulfides were converted to the corresponding thiosulfinate (Eq 2 and 4) by oxidation, using *m*-chloroperoxybenzoic acid, to provide our target thiosulfinates.

The formation of thiosulfonates (R_1-S-SO_2-R_2) was totally avoided when the reactions were performed at -78 °C[55]. TLC and NMR analysis of the crude reaction mixtures confirmed the absence of thiosulfonate formation at this temperature (data not shown). Crude thiosulfinate mixtures were purified by flash column chromatography, with ethyl acetate and *n*-hexane used as an eluent. The structures of the final compounds **1b–22b** (Figure 1) were confirmed by analysis of their spectral and analytical data (Supplementary material). Compounds **11b** and **12b** were produced from the oxidation of compound **11a**, and due to their almost identical physical properties, separation was not possible during the purification step. **11b** and **12b**, formed at a ratio of 4:3, were treated as a mixture and will, for simplicity, henceforth be collectively referred to as **11b**. To evaluate degradation associated with the storage conditions, compounds **7b** and **8b** were dissolved in chloroform and stored at room temperature for 3 weeks.

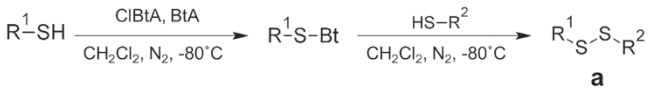

Eq 3

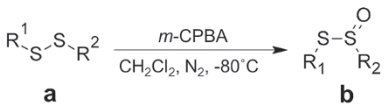

Eq 4

Compound	R_1	R_2
7	4-CH_3Ph	CH_3CH_2
8	4-CH_3Ph	$CH_3CH_2CH_2$
9	4-CH_3Ph	*t*-Bu
10	4-CH_3Ph	4-(*t*-Bu)PhCH_2
11	4-OCH_3Ph	4-CH_3Ph
12	4-CH_3Ph	4-OCH_3Ph
14	4-OCH_3Ph	CH_3CH_2
15	4-OCH_3Ph	$CH_3(CH_2)_2CH_2$
16	4-OCH_3Ph	*t*-Bu
17	4-OCH_3Ph	$CH_3(CH_2)_4CH_2$
18	4-OCH_3Ph	C_6H_{10}
19	4-OCH_3Ph	4-(*t*-Bu)PhCH_2
21	4-OHPh	$CH_3(CH_2)_2CH_2$
22	4-OHPh	$CH_3(CH_2)_4CH_2$

Scheme 2. Synthetic methods for the preparation of asymmetric thiosulfinates **7b–12b**, **14b–19b** and **21b–22b**.

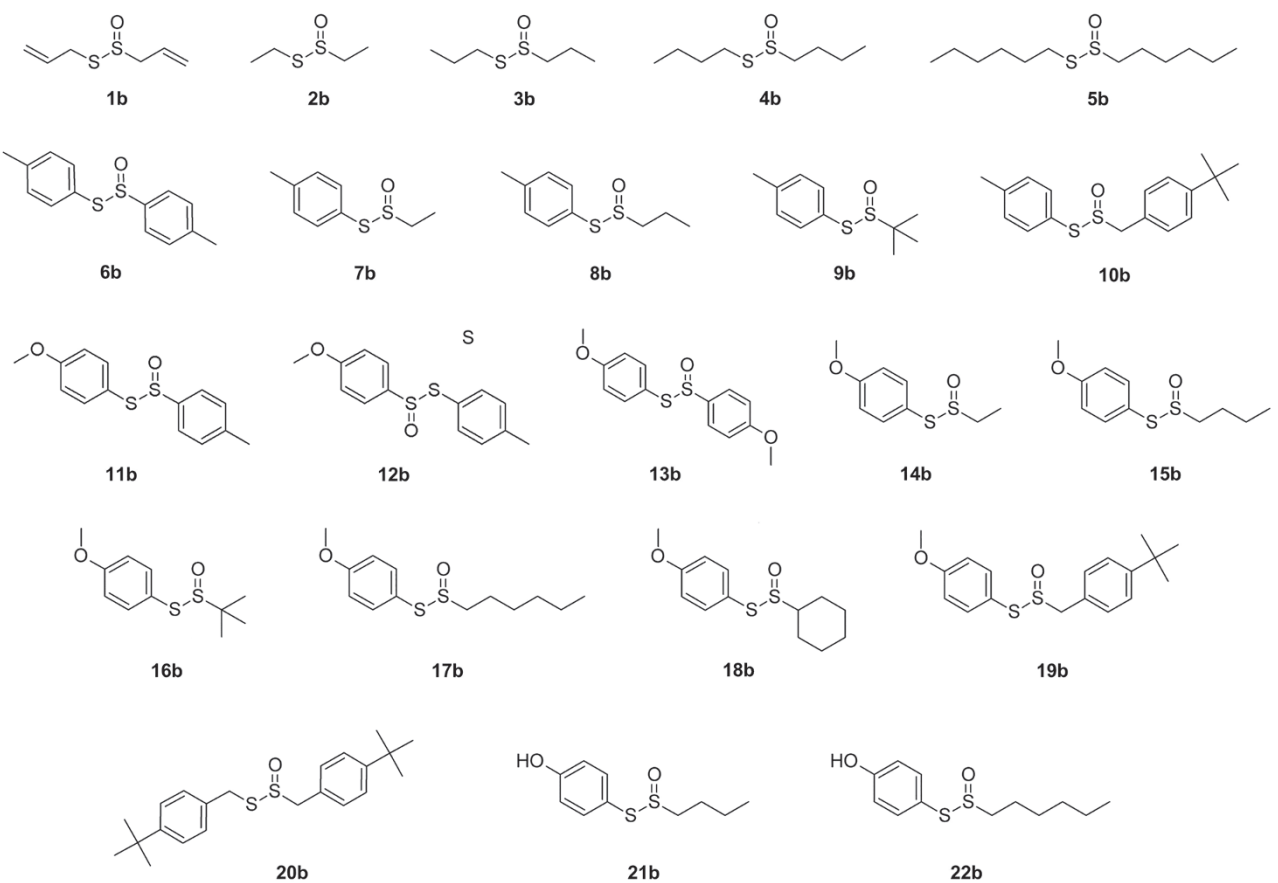

Figure 1. Chemical structures of synthesised thiosulfinates.

Spectral analysis did not show decomposition, but allicin stored under similar conditions showed a significant increase in degradation by-products (data not shown). Compound **13b** was also found to be significantly more stable than allicin. Spectral analysis of pure **13b** did not show signs of decomposition after >12 months of storage at room temperature (data not shown).

The half-life of allicin is drastically increased when stored at -80 °C, with no detectable loss of purity after 24 months of storage at this temperature[56]. Consequently, all compounds were stored under these conditions until required. The stability of thiosulfinates is significantly improved when dissolved in polar solvents; therefore, all working stock solutions were dissolved in DMSO and stored at -20 °C[57]. To ensure that these compounds were suitable for biological application, we analyzed each with OSIRIS Property Explorer to determine the toxicity risks and drug-likeness of each molecule (Supplementary material, Table S1). Each compound was found to be free of any toxicity risks, with all compounds free of mutagenic, tumorigenic, reproductive or irritant-like effects. Of the compounds tested, only **20b** had Lipinski violations, due to a high predicted LogP and poor solubility, indicating that poor absorption or poor permeability is likely[58]. This compound did show some anticancer activity against both MCF-7 and Dx cells (Supplementary material); however, in agreement with the OSIRIS prediction, it was poorly soluble in both DMSO and aqueous solutions and as such was excluded from further testing.

In vitro anticancer activity

The *in vitro* antiproliferative activities of the prepared compounds were evaluated against MCF-7 and MCF-7/Dx cells. All thiosulfinates were initially screened at a single high dose (50 μmol/L). Compounds that satisfied a predetermined level of cellular viability (<50%), relative to a vehicle control, were selected for further analysis.

It has previously been shown that after 24 h of incubation in water at 37 °C at a pH of 7.5, only 62% of pure allicin remains in a test sample[59]. Therefore, for the 72-h viability assays, the cell culture media was replaced daily with fresh allicin medium. This considerably improved anticancer activity against both cell lines compared to experiments in which cells were treated in the same allicin stock for 72 h (Supplementary material).

In preliminary screenings, compounds allicin**, 4b**, **7b**, **8b**, **11b**, and **13b–19b** showed pronounced growth inhibition against MDR Dx cells at 50 μmol/L. However, at the same concentration, only allicin and **13b** reduced the cellular viability of MCF-7 cells below 50%. The thiosulfinate derivatives showed pronounced selectivity towards the MDR Dx cells compared to the drug-sensitive MCF-7 cells (Figure 2A).

Amongst the aromatic thiosulfinates, there was a clear correlation between anticancer activity and the substituent attached to the sulfenyl sulfur (R_1), with the more electron-rich 4-methoxybenzyl group showing higher antiproliferative effects compared to the 4-methylbenzyl group (Figure 2B).

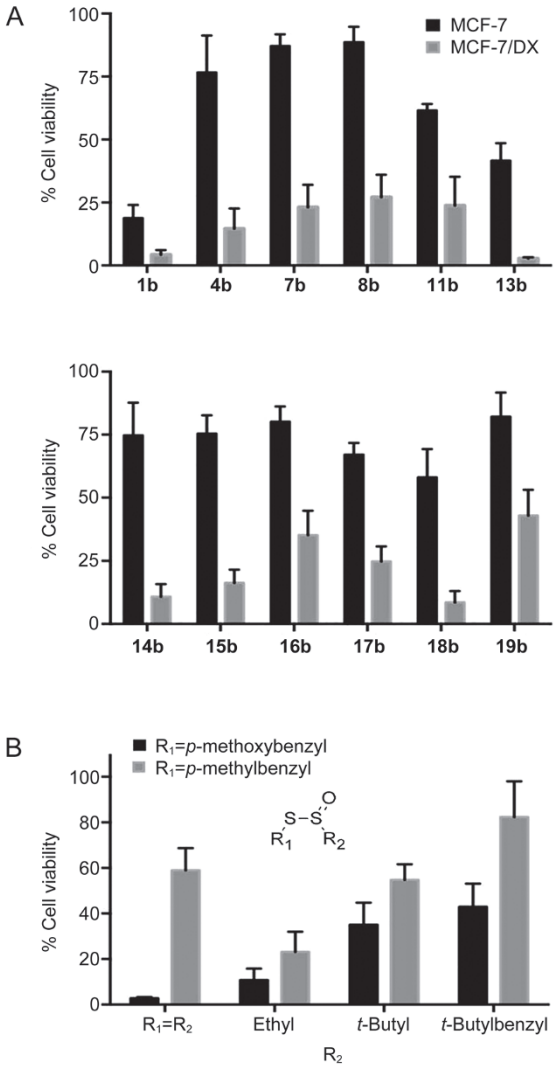

Figure 2. Antiproliferative activity of thiosulfinates. (A) Specificity of compounds **1b**, **4b**, **7b**, **8b**, **11b** and **13b–19b** at 50 μmol/L towards MDR MCF-7/Dx cells, compared to drug sensitive MCF-7 cells. (B) Comparison of molecule potency at 50 μmol/L towards MCF/Dx cells, where side chain R_2 is conserved and electron donating functional group (R_1) is altered. Data represents the mean±SEM of at least 3 independent experiments.

Additionally, for the asymmetric thiosulfinates, the longer and/or bulkier the substituent on the sulfinyl sulfur (R_2), the less potent the compound's anticancer activity. This trend was also apparent at lower concentrations (Supplementary material). Accordingly, **4b**, **7b**, **8b**, **11b**, and **13a–19b** were selected for further analysis. The IC_{50} values of allicin, **4b**, **7b**, **8b**, **11b**, and **13a–19b** were determined and are summarized in Table 1. As with the initial screening, the compounds with the most electron-rich group on the sulfenyl sulfur exhibited stronger antiproliferative activity, with **13b** (both R groups occupied by the 4-methoxybenzyl moiety) exhibiting the greatest anticancer activity in both MCF-7 and Dx cells. Due to its promising cytotoxic activity against both MCF-7 and Dx cells, **13b** was selected for further studies.

Table 1. *In-vitro* anticancer activity (IC_{50})[a] of selected active molecules.

Compound	MCF-7/Dx IC_{50} (μmol/L)	MCF-7 IC_{50} (μmol/L)
Allicin	41.23±0.52	–[b]
4b	33.74±2.38	>50
7b	35.99±0.82	>50
8b	38.11±1.46	>50
11b	40.77±3.18	>50
13b	18.54±0.24	46.50±1.98
14b	28.97±1.78	>50
15b	28.97±1.31	>50
16b	45.54±2.68	>50
17b	41.11±2.08	>50
18b	28.75±0.38	>50
19b	48.61±3.57	>50

[a] 50% inhibitory concentration after 72 h of treatment.
[b] Not reported.

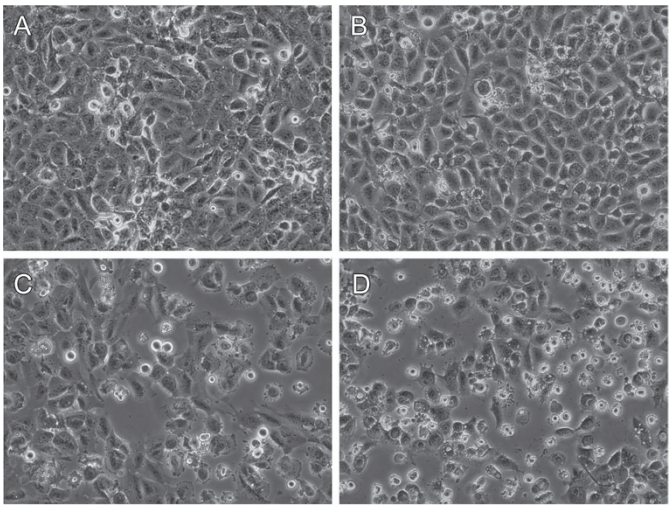

Figure 3. Effects of thiosulfinate **13b** on the cellular morphology and viability of MCF-7/Dx cells. Images show morphological changes in MCF-7/Dx cells treated for 24 h with (A) vehicle control, (B) 25 μmol/L, (C) 37.5 μmol/L and (D) 50 μmol/L. There was no decrease in cell viability at 12.5 μmol/L (98.33%±1.86%), a slight decrease at 25 μmol/L (91.75%±4.31%), and significant decreases at 37.5 μmol/L and 50 μmol/L (43.13%±2.07% and 27.29%±5.79%, respectively). Data and images represent the mean± SEM of 3 independent experiments.

Cellular morphology

To observe the effects of thiosulfinate treatment on cellular morphology, MCF-7/Dx cells were treated with various concentrations of **13b** for 24 h. The morphology of Dx cells treated with 25 μmol/L **13b** was not significantly affected after 24 h. However, at 37.5 and 50 μmol/L, cells displayed distinct membrane blebbing, cell shrinkage, detachment and an apparent disaggregation (Figure 3). This reduction in viable cells was confirmed using the Trypan blue exclusion assay, which after treatment with 37.5 and 50 μmol/L **13b** resulted in a cell viability reduction to 43.13%±2.07% and 27.29%±5.79%, respectively.

Cell cycle analysis

Many cytotoxic compounds inhibit cell growth by arresting cells at particular stages in the cell cycle. To investigate whether the synthesized thiosulfinates had this effect, MCF-7/Dx cells were incubated with various concentrations of **13b** for 24 h and then stained with PI as described above in the Materials and Methods section. Consistent with its effect on cell growth inhibition, **13b** caused cell cycle arrest in Dx cells in a dose-dependent manner (Figure 4). Cells treated with the vehicle control showed a typical distribution of 44.30% of cells in the G_0/G_1 phase, 38.13% in the S phase, and 16.70% of cells in the G_2/M phase (Table 2). Treatment of cells with 12.5 μmol/L **13b** increased the proportion of cells in the G_0/G_1 phase to 50.54% and caused a small decrease in cells in the S phase. At 37.5 μmol/L and 50 μmol/L, there were reductions in the proportion of cells in the G_0/G_1 and S phases, while the number of cells in G_2/M increased significantly. After being treated with 50 μmol/L, 29.37% of cells were found to be in the G_0/G_1 phase, 26.17% in the S phase, and 44.83% arrested in the G_2/M phase. During the screening, many thiosulfinates were also found to significantly arrest Dx cells in the G_2/M phase (Supplementary material). These data demonstrate that

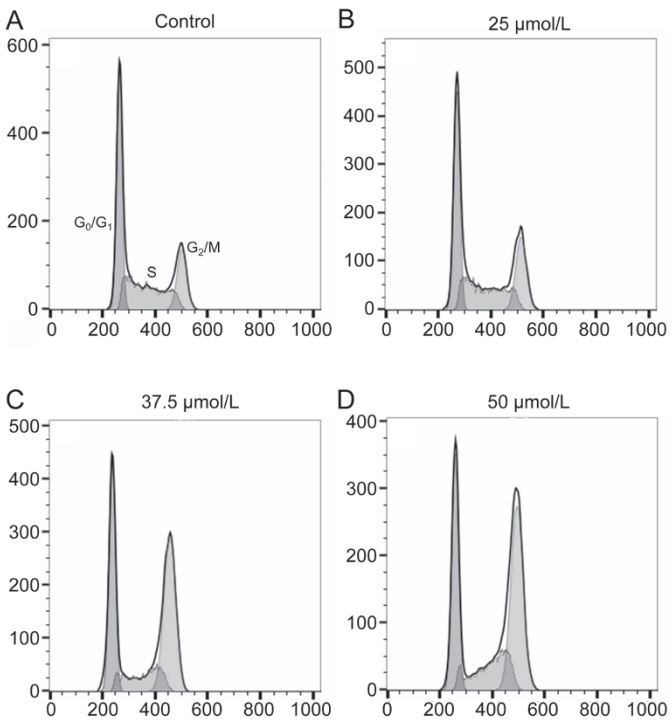

Figure 4. Effect of **13b** on the cell cycle progression of MCF-7/Dx cells. Cells were treated for 24 h with (A) DMSO (vehicle control), (B) 25 μmol/L, (C) 37.5 μmol/L and (D) 50 μmol/L. Images are representative of 4 independent experiments.

Table 2. Effect of compound **13b** on the cell cycle progression of MCF-7/Dx cells[a]. $^{*}P<0.05$, $^{**}P<0.01$ compared with the indicated compound to control cells in the corresponding cell cycle phase.

Conc (μmol/L)	G_0/G_1 phase (%)	S phase (%)	G_2/M phase (%)
Control	44.30±0.76	38.13±0.57	16.70±0.77
12.5	50.54±2.07	33.24±1.99	15.42±0.77
25	39.66±4.78	28.94±1.53*	30.46±6.06**
37.5	32.40±1.33*	26.90±3.56*	40.00±2.95**
50	29.37±3.37**	26.17±2.80**	44.83±3.19**

[a] MCF-7/Dx cells were treated with compound **13b** then cell cycle distribution was analysed after staining with PI. Results are expressed as the percentage of cells in each phase of the cell cycle, data represents the mean±SEM of 4 independent experiments.

synthesized thiosulfinates primarily arrest Dx cells in the G_2/M phase, significantly reducing the proportion of cells in the G_0/G_1 and S phases.

Induction of apoptosis

The translocation of phospholipid phosphatidylserine (PS) to the outer leaflet of the cell plasma membrane is one of the hallmarks of apoptosis[60]. This is followed by a loss of membrane integrity and eventual cell death. To establish whether thiosulfinates induce cell death via this mechanism, MCF-7/Dx cells were treated with 12.5–50 μmol/L of **13b** for 24 h and then stained with Annexin V-450 (which binds to exposed PS) and PI to determine the proportion of cells undergoing early apoptosis (Annexin-positive, PI-negative), late apoptosis (Annexin-positive, PI-positive), and total apoptosis (early+late apoptosis) (Figure 5).

At 12 μmol/L, there was no significant increase in the total number of apoptotic cells relative to the solvent control. A small increase was observed in cells treated with 25 μmol/L, and significant increases were observed in Dx cells treated with 37.5 and 50 μmol/L **13b**. The proportion of cells undergoing apoptosis at 25 μmol/L, 37.5 μmol/L and 50 μmol/L was 7.06%±0.82%, 31.32%±8.06% and 57.52%±2.92%, respectively, indicating that **13b** induces apoptosis in a dose-dependent manner (Table 3).

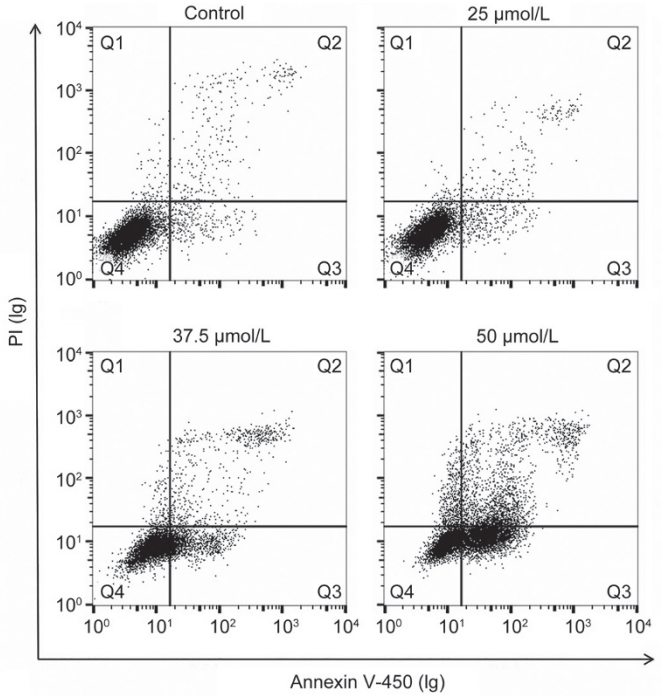

Figure 5. Effect of compound **13b** on the induction of apoptosis in MCF-7/Dx cells. MCF-7/Dx cells were treated with various concentrations of **13b** for 24 h, stained with Annexin V-450 and PI, and the apoptotic effect was assessed by flow cytometry. Representative results are shown, with quadrants indicating the proportion of cells that are necrotic: Q1, late apoptotic: Q2, early apoptotic: Q3, and viable: Q4. Images are representative of 3 independent experiments.

Measurement of mitochondrial function

Mitochondria play a central role in many biological processes, especially in the initiation of apoptosis. To further investigate the cytotoxic effects of thiosulfinates on MCF-7/Dx cells, we sought to determine whether **13b** disrupted mitochondrial respiratory function, which was investigated using the XF24 extracellular flux analyzer. As allicin has previously been shown to interfere with mitochondrial functions in various cell lines, including MCF-7, we included it for comparison[25, 29].

Dx cells were treated with 10–50 μmol/L of allicin and **13b** for 24 h, with both OCR and extracellular acidification rate (ECAR) measured using the "mitochondrial stress test" (Agi-

Table 3. Quantitative apoptosis assay of MCF-7/Dx cells treated with **13b**[a]. $^{**}P<0.01$ *vs* the % of apoptotic cells of the control.

Compound	(μmol/L)	Viable cells (Q4, %)	Early apoptotic cells (Q3, %)	Late apoptotic cells (Q2, %)	Necrotic cells (Q1, %)	Apoptotic cells (Q2+Q3, %)
Control	0	96.89±0.48	1.48±0.22	1.03±0.23	0.60±0.11	2.51±0.45
13b	12.5	94.65±0.65	2.16±0.10	1.95±0.27	1.24±0.25	4.10±0.36
13b	25	91.88±0.81	3.93±0.09	3.13±0.87	1.05±0.26	7.06±0.82
13b	37.5	62.58±7.34	18.97±6.88	12.35±1.85	6.07±2.15	31.32±8.06**
13b	50	36.85±3.33	33.35±1.87	24.17±2.92	5.61±0.66	57.52±2.92**

[a] MCF-7/Dx cells were treated with various concentrations of **13b** for 24 h, the apoptotic affect was assessed by flow cytometry after staining with Annexin V-450 and PI. Data represents the mean±SEM of 3 independent experiments.

lent Technologies, CA, USA). Sequential addition of the mitochondrial complex inhibitors oligomycin, FCCP, antimycin A and rotenone allowed for the determination of several mitochondrial function parameters. Treatment with allicin and **13b** inhibited the basal OCR relative to the vehicle control in a dose-dependent manner (Figure 6). The addition of oligomycin, an ATP synthase inhibitor, allows for the determination of ATP-linked respiration, with both allicin and **13b** inducing a decrease. The addition of FCCP, an electron transport chain uncoupler, allows for the measurement of maximum cellular respiration rate in response to increased energy demand. There was a significant dose-dependent decrease observed for both compounds. Likewise, spare respiratory capacity was significantly impaired after treatment with both thiosulfinates.

When cells lose the ability to maintain oxidative phosphorylation/respiration, they often compensate by increasing glycolysis to maintain ATP production[61]. Due to the decrease observed in the OCR, we investigated the effects of allicin and **13b** on the ECAR, a surrogate marker for glycolysis[62]. The glycolytic potential was also measured by the addition of oligomycin, which forces the cells to compensate by increasing glycolysis (Supplementary material). Despite decreases in the OCR at all tested concentrations, there was no significant effect on basal ECAR or glycolytic potential.

Discussion

Allicin has numerous health benefits and has been shown to be effective against many diseases. Use as a therapeutic agent is limited, however, due to a propensity for allicin to degrade under relatively mild conditions. In considering this, we developed a library of allicin derivatives and assessed their anticancer activity against the breast adenocarcinoma cell line MCF-7 and the MDR sub-line MCF-7/Dx. In an effort to stabilize the functionality of the thiosulfinate group, we substituted the labile allylthio moiety with various substituents. Spectral analysis of aryl thiosulfinates stored in chloroform at room temperature for several weeks showed minimal decomposition, while allicin showed distinct increases in impurities (data not shown). Additionally, compound **13b** was found to be stable after storage at room temperature for over a year, whereas allicin is known to be incredibly unstable when stored in its pure state under these conditions[63]. These results reflect previous findings that electron-rich aryl-substituted thiosulfinates are much more stable than allicin under similar condi-

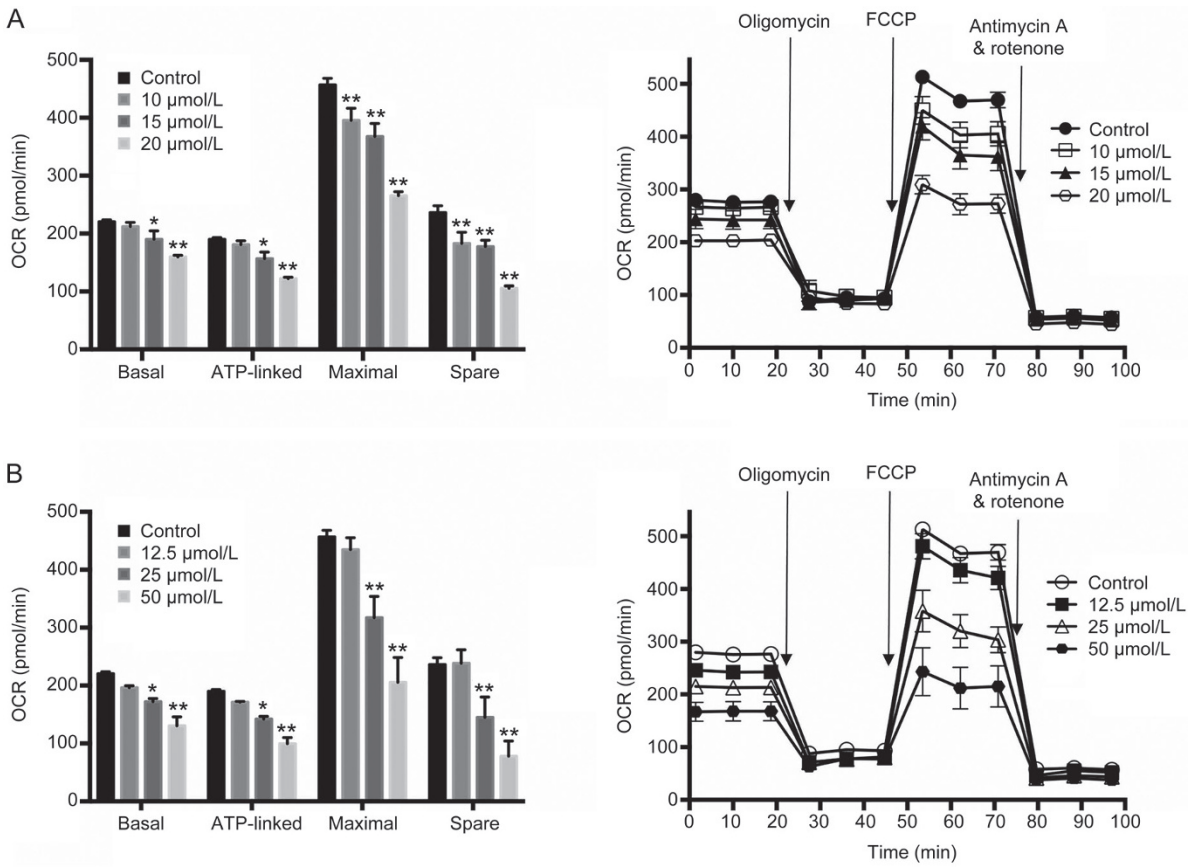

Figure 6. Effect of thiosulfinates on mitochondrial function. Cells were seeded in XF24 well plates and treated for 24 h with (A) **13b** and (B) allicin at the indicated concentrations. Medium was then replaced with unbuffered XF assay medium, supplemented with sodium pyruvate, glucose and *L*-glutamine, and allowed to equilibrate for 1 h. Baseline measurements were recorded then oligomycin, FCCP, antimycin A and rotenone were injected sequentially at the indicated time points. Data represents the mean±SEM of at least 4 independent experiments. $^{*}P<0.05$, $^{**}P<0.01$, compared with the indicated compound to the vehicle control.

tions[40, 57]. These results were also reflected in our 72-h antiproliferative assay (Figure 2A). The majority of thiosulfinates tested showed improved activity compared to cells incubated with allicin, which we propose is in part due to the increased stability of these compounds. To maintain activity for the duration of the assay, allicin was replenished with fresh stock and media every 24 h. Conversely, when incubated with the same allicin stock for 72 h, cell viability remained largely unaffected in both cell lines (Supplementary material). This suggests that the antiproliferative activity observed in this assay is due to allicin and not its degradation by-products.

Increasing the chain length of the symmetric alkyl thiosulfinates showed a corresponding reduction in the proportion of viable cells in both cell lines. However, when one alkyl chain was replaced with a benzyl functional group, the compounds with shorter and less bulky alkyl groups showed more favorable results, with compounds containing the 4-methoxybenzyl moiety showing the greatest activity (Figure 2). We propose that this improved activity of the benzyl group over the straight chain substituents is due in part to the benzyl group acting as a bioisostere for the allyl group.

Several thiosulfinate derivatives exhibited cytotoxic activity towards Dx cells (Table 1). However, of the compounds tested, only **13b** displayed an IC_{50} <50 μmol/L in MCF-7 cells. These results highlight the disparity in the anticancer activity (IC_{50}) of the thiosulfinates against the drug-sensitive MCF-7 cells *vs* MDR Dx cells. Since Dx cells express P-gp, it was expected that they would be less sensitive to treatment, as Dx cells exhibit up to a 200-fold resistance to conventional chemotherapeutics *in vitro*[64].

A possible explanation for this selectivity could be linked to caspase-3 expression. MCF-7 cells do not express caspase-3, a key player in the apoptosis cascade[65]. Conversely, Dx cells do express caspase-3 and, in direct comparison with MCF-7 cells, have been shown to be significantly more susceptible to certain apoptotic stimuli[64, 66]. Whether this accounts for the disparity in the anticancer activity shown in Table 1 is currently unknown. As allicin has been shown to initiate apoptosis through both caspase-dependent and caspase-independent mechanisms in various cell lines[27, 67], further work is required to determine whether Dx cell death is executed via this pathway.

Allicin has previously been shown to be cancer specific, inducing significantly lower levels of cytotoxicity against normal cells[18, 25, 35]. Additionally, short chain thiosulfinates, containing both allyl and saturated chains, show good activity *in vivo*, significantly increasing the survival times of sarcoma-bearing mice[36]. Our most potent molecule, **13b**, did not show specificity toward cancer cells, with effects observed in non-malignant human brain epithelial cells (HBEC) (Supplementary material). Interestingly, when treated with allicin, HBEC cells showed levels of cytotoxicity similar to those observed in Dx cells (data not shown), despite the numerous reports of allicin's cancer-specific activity. In light of this, we are currently undertaking further studies to improve the specificity of these molecules through modification of the pharmacophore. Additionally, it would be interesting to investigate the anticancer effect of these molecules on hematological cell lines, as it has previously been shown that allicin is more toxic to cells in suspension compared to cells in monolayers[68].

Allicin has previously been shown to rapidly induce morphological changes in colon carcinoma cells, gastric cancer cells and MCF-7 breast cancer cells, as well as reduce cell proliferation and induce growth arrest[26, 69, 70]. Similarly, the thiosulfinates described in this study altered Dx cellular morphology. Cell shrinkage, detachment, and fragmentation were observed 24 h after treatment (Figure 3). This change in morphology was evident as early as 6 h after initial treatment (Supplementary material). To further investigate the mechanisms behind this reduced viability and altered cellular morphology, we tested for apoptosis, as allicin and saturated short-chain thiosulfinates have been shown to induce apoptosis in a number of cell lines[26–28]. In the present study, thiosulfinates were found to induce apoptosis in Dx cells to varying degrees (Supplementary material), with **13b** showing the most activity, inducing apoptosis in a dose-dependent manner (Table 3).

The effect of allicin on viability and apoptosis has been linked to a reduction in intracellular GSH, which indicates an alteration in the cellular redox state[25, 28, 71]. GSH reduction occurs in response to sustained production of ROS upon exposure to allicin, which then leads to a decrease in mitochondrial potential, a reduction in ATP generation and subsequent cell death[16, 29, 72]. ROS are generated in cells under normal conditions; however, production is elevated when there is a disruption either in the electron transport chain or ATP generation. Tumor cells inherently show elevated metabolic activity and oxygen consumption and produce high levels of ROS under normal conditions, making them more susceptible to damage from excess ROS production[73, 74]. As mitochondria are major mediators of apoptosis and cellular bioenergetics, modulation of mitochondrial respiratory function in an effort to kill cancer cells is attracting interest as a therapeutic strategy[74–76]. To investigate the possible mitochondrial effects of the synthesized thiosulfinates on Dx cells, we used the XF24 extracellular flux analyzer, allowing for the measurement of multiple parameters associated with mitochondrial function[77].

In this study, we found that allicin and compound **13b** cause similar responses in Dx cells, with significant reductions in oxygen consumption both at basal levels and under stress, as well as a decrease in ATP turnover (Figure 6). This suggests that these compounds reduce the cell's ability to generate a membrane potential and its capacity to synthesize ATP[77]. Spare respiratory capacity was also significantly impaired after treatment with both thiosulfinates, which indicates a loss of mitochondrial membrane potential as well as a significantly reduced capacity to respond to stressors, such as ROS[78, 79]. We hypothesize that these compounds damage the mitochondrial electron transport chain through an elevation in ROS, which initiates the apoptosis cascade leading to cell death. Our investigations are ongoing to determine the precise molecular mechanisms underlying this process.

These disruptions to mitochondrial respiration offer another possible explanation for the observed sensitivity of MDR Dx cells to thiosulfinate treatment relative to the drug-sensitive MCF-7 cells. Dx cells may be more susceptible to thiosulfinate treatment due to the effects of a phenomenon known as collateral sensitivity. Collateral sensitivity is the ability of a compound to preferentially kill MDR cells over drug-sensitive cells and is generally associated with the over-expression of P-gp[80]. Various mechanisms have been proposed for the effects of CS, such as the down-regulation of P-gp expression, disruption of oxygen consumption, elevated ROS, and depletion of cellular ATP[81–83]. CS is represented as a ratio, which is determined by dividing the IC_{50} of the MDR sub-line by the IC_{50} of the drug-sensitive parental line to produce a resistance ratio ≤0.5[84]. For **13b**, the IC_{50} was 46.50 μmol/L for MCF-7 cells and 18.54 mmol/L for Dx cells, providing a resistance ratio of 0.40. In conjunction with the ability of **13b** to reduce ATP-linked respiration and to disrupt OCR under stress and at basal levels, this result suggests that **13b** is a potential CS agent.

Garlic-derived compounds, including allicin, are known to inhibit cancer cell growth by disrupting the cell cycle, causing cells to accumulate predominately in the G_2/M phase in direct response to the overproduction of ROS and disruption to mitochondrial respiration[85, 86]. Treatment with compound **13b** resulted in a dose-dependent accumulation of cells in G_2/M (Table 2). Additionally, during initial screenings at 50 μmol/L, the cell cycle was found to be arrested at the G_2/M phase for most of the thiosulfinates tested (Supplementary material). For allicin, we did not find any change in cell cycle distribution at this concentration; however, higher concentrations increased accumulation in G_0/G_1 and G_2/M, with these results reflecting a previous study on MCF-7 cells[25].

In addition to antiproliferative effects, thiosulfinates have also shown promise as antimetastatic agents. It has recently been reported that blocking mitochondrial ATP production inhibits breast cancer cell migration and invasion. Likewise, allicin has been shown to induce cell cycle arrest through microtubule disruption and to suppress invasion and metastasis of breast cancer *in vitro*[30, 70, 87]. As we have shown that allicin and **13b** inhibit ATP-linked mitochondrial respiration, we hypothesize that these compounds are likely to influence cellular migration and therefore warrant further investigation.

In conclusion, allicin has previously been shown to exhibit many beneficial biological effects, including strong anticancer activity. In light of the instability of allicin *in vitro* and *in vivo*, we sought to improve its activity by developing a library of thiosulfinate derivatives with increased half-life and improved efficacy. We found that these thiosulfinate derivatives have improved antiproliferative activity in drug-sensitive and MDR breast cancer cell lines. Several compounds showed specificity for the MDR cells, and Dx cells showed collateral sensitivity to treatment with **13b**. We report that these derivatives alter cellular morphology, induce apoptosis and cell cycle arrest, and inhibit mitochondrial bioenergetics, presenting a promising lead for future studies in the treatment of MDR cancer.

Author contribution

Mary BEBAWY and Alison UNG designed the research; Ariane ROSEBLADE performed the research; Ariane ROSEBLADE, Mary BEBAWY and Alison UNG analyzed the data and wrote the paper.

Supplementary information

Supplementary information is available at Acta Pharmacologica Sinica's website

References

1 Torre LA, Bray F, Siegel RL, Ferlay J, Lortet–Tieulent J, Jemal A. Global cancer statistics, 2012. CA Cancer J Clin 2015; 65: 87–108.
2 Szakács G, Paterson JK, Ludwig JA, Booth-Genthe C, Gottesman MM. Targeting multidrug resistance in cancer. Nat Rev Drug Discov 2006; 5: 219–34.
3 Longley DB, Johnston PG. Molecular mechanisms of drug resistance. J Pathol 2005; 205: 275–92.
4 Sharom FJ, Yu X, Doige CA. Functional reconstitution of drug transport and ATPase activity in proteoliposomes containing partially purified P-glycoprotein. J Biol Chem 1993; 268: 24197–202.
5 Breuninger LM, Paul S, Gaughan K, Miki T, Chan A, Aaronson SA, *et al.* Expression of multidrug resistance-associated protein in NIH/3T3 cells confers multidrug resistance associated with increased drug efflux and altered intracellular drug distribution. Cancer Res 1995; 55: 5342–7.
6 Leonard GD, Fojo T, Bates SE. The role of ABC transporters in clinical practice. Oncologist 2003; 8: 411–24.
7 Tiwari AK, Sodani K, Dai CL, Ashby CR, Chen ZS. Revisiting the ABCs of multidrug resistance in cancer chemotherapy. Curr Pharm Biotechnol 2011; 12: 570–94.
8 Saab AM, Guerrini A, Zeino M, Wiench B, Rossi D, Gambari R, *et al. Laurus nobilis* L. seed extract reveals collateral sensitivity in multidrug-resistant p-glycoprotein-expressing tumor cells. Nutr Cancer 2015; 67: 664–75.
9 Huang TH, Bebawy M, Tran VH, Roufogalis BD. Specific reversal of multidrug resistance to colchicine in CEM/VLB 100 cells by Gynostemma pentaphyllum extract. Phytomedicine 2007; 14: 830–9.
10 Tran VH, Marks D, Duke RK, Bebawy M, Duke CC, Roufogalis BD. Modulation of P-glycoprotein-mediated anticancer drug accumulation, cytotoxicity, and ATPase activity by flavonoid interactions. Nutr Cancer 2011; 63: 435–43.
11 Block E. The organosulfur chemistry of the genus allium–implications for the organic chemistry of sulfur. Angew Chem Int Ed Engl 1992; 31: 1135–78.
12 Park EK, Kwon KB, Park KI, Park BH, Jhee EC. Role of Ca^{2+} in diallyl disulfide-induced apoptotic cell death of HCT-15 cells. Exp Mol Med 2002; 34: 250–7.
13 Herman-Antosiewicz A, Singh SV. Signal transduction pathways leading to cell cycle arrest and apoptosis induction in cancer cells by Allium vegetable-derived organosulfur compounds: a review. Mutat Res 2004; 555: 121–31.
14 Xu YS, Feng JG, Zhang D, Zhang B, Luo M, Su D, *et al.* S-allylcysteine, a garlic derivative, suppresses proliferation and induces apoptosis in human ovarian cancer cells *in vitro*. Acta Pharmacol Sin 2014; 35: 267–74.
15 Chung LY. The antioxidant properties of garlic compounds: allyl cysteine, alliin, allicin, and allyl disulfide. J Med Food 2006; 9: 205–13.
16 Corral MJ, Benito-Peña E, Jiménez-Antón MD, Cuevas L, Moreno-

Bondi MC, Alunda JM. Allicin induces calcium and mitochondrial dysregulation causing necrotic death in leishmania. PLoS Negl Trop Dis 2016; 10: e0004525.
17 Waag T, Gelhaus C, Rath J, Stich A, Leippe M, Schirmeister T. Allicin and derivates are cysteine protease inhibitors with antiparasitic activity. Bioorg Med Chem Lett 2010; 20: 5541–3.
18 Ilić D, Nikolić V, Ćirić A, Soković M, Stanojković T, Kundaković T*, et al.* Cytotoxicity and antimicrobial activity of allicin and its transformation products. Med Plant Res 2012; 6: 59–65.
19 Cañizares P, Gracia I, Gómez LA, de Argila CM, Boixeda D, García A*, et al.* Allyl-thiosulfinates, the bacteriostatic compounds of garlic against *Helicobacter pylori*. Biotechnol Prog 2004; 20: 397–401.
20 Briggs WH, Xiao H, Parkin KL, Shen C, Goldman IL. Differential inhibition of human platelet aggregation by selected allium thiosulfinates. J Agric Food Chem 2000; 48: 5731–35.
21 Dirsch VM, Kiemer AK, Wagner H, Vollmar AM. Effect of allicin and ajoene, two compounds of garlic, on inducible nitric oxide synthase. Atherosclerosis 1998; 139: 333–39.
22 Cha JH, Choi YJ, Cha SH, Choi CH, Cho WH. Allicin inhibits cell growth and induces apoptosis in U87MG human glioblastoma cells through an ERK-dependent pathway. Oncol Rep 2012; 28: 41.
23 Wang Z, Liu Z, Cao Z, Li L. Allicin induces apoptosis in EL-4 cells *in vitro* by activation of expression of caspase-3 and-12 and up-regulation of the ratio of Bax/Bcl-2. Nat Prod Res 2012; 26: 1033–7.
24 Lee J, Gupta S, Huang JS, Jayathilaka LP, Lee BS. HPLC–MTT assay: Anticancer activity of aqueous garlic extract is from allicin. Anal Biochem 2013; 436: 187–9.
25 Hirsch K, Danilenko M, Giat J, Miron T, Rabinkov A, Wilchek M*, et al.* Effect of purified allicin, the major ingredient offreshly crushed garlic, on cancer cell proliferation. Nutr Cancer 2000; 38: 245–54.
26 Sun L, Wang X. Effects of allicin on both telomerase activity and apoptosis in gastric cancer SGC-7901 cells. World J Gastroenterol 2003; 9: 1930–4.
27 Oommen S, Anto RJ, Srinivas G, Karunagaran D. Allicin (from garlic) induces caspase-mediated apoptosis in cancer cells. Eur J Pharmacol 2004; 485: 97–103.
28 Miron T, Wilchek M, Sharp A, Nakagawa Y, Naoi M, Nozawa Y*, et al.* Allicin inhibits cell growth and induces apoptosis through the mitochondrial pathway in HL60 and U937 cells. J Nutr Biochem 2008; 19: 524–35.
29 Chu YL, Ho CT, Chung JG, Raghu R, Lo YC, Sheen LY. Allicin induces anti-human liver cancer cells through the p53 gene modulating apoptosis and autophagy. J Agric Food Chem 2013; 61: 9839–48.
30 Lee CG, Lee HW, Kim BO, Rhee DK, Pyo S. Allicin inhibits invasion and migration of breast cancer cells through the suppression of VCAM-1: Regulation of association between p65 and ER-α. J Funct Foods 2015; 15: 172–85.
31 Bebawy M, Combes V, Lee E, Jaiswal R, Gong J, Bonhoure A*, et al.* Membrane microparticles mediate transfer of P-glycoprotein to drug sensitive cancer cells. Leukemia 2009; 23: 1643–9.
32 Rendu F, Brohard-Bohn B, Pain S, Bachelot-Loza C, Auger J. Thiosulfinates inhibit platelet aggregation and microparticle shedding at a calpain-dependent step. Thromb Haemost 2001; 86: 1284–91.
33 Roseblade A, Luk F, Ung A, Bebawy M. Targeting microparticle biogenesis: a novel approach to the circumvention of cancer multidrug resistance. Curr Cancer Drug Targets 2015; 15: 205–14.
34 Roseblade A, Luk F, Rawling T, Ung A, Grau GE, Bebawy M. Cell-derived microparticles: new targets in the therapeutic management of disease. J Pharm Pharm Sci 2013; 16: 238–53.
35 Ghazanfari T, Yaraee R, Rahmati B, Hakimzadeh H, Shams J, Jalali-Nadoushan MR. *In vitro* cytotoxic effect of garlic extract on malignant and nonmalignant cell lines. Immunopharmacol Immunotoxicol 2011; 33: 603–8.
36 Park KW, Kim SY, Jeong IY, Byun MW, Park KH, Yamada K*, et al.* Cytotoxic and antitumor activities of thiosulfinates from *Allium tuberosum* L. J Agric Food Chem 2007; 55: 7957–61.
37 Block E, Ahmad S, Catalfamo JL, Jain MK, Apitz-Castro R. Antithrombotic organosulfur compounds from garlic: structural, mechanistic, and synthetic studies. J Am Chem Soc 1986; 108: 7045–55.
38 Cavallito CJ, Bailey JH. Allicin, the antibacterial principle of *Allium sativum* I. Isolation, physical properties and antibacterial action. J Am Chem Soc 1944; 66: 1950–1.
39 Small LD, Bailey JH, Cavallito CJ. Alkyl thiolsulfinates. J Am Chem Soc 1947; 69: 1710–3.
40 Stellenboom N, Hunter R, Caira MR, Bourne SA, Cele K, Qwebani T*, et al.* Synthesis and inclusion of S-aryl alkylthiosulfinates as stable allicin mimics. ARKIVOC 2007; 9: 53–63.
41 Hughes TV, Hammond SD, Cava MP. A convenient new synthesis of 1-cyanobenzotriazole and its use as a C-cyanating reagent. J Org Chem 1998; 63: 401–2.
42 Natarajan P, Sharma H, Kaur M, Sharma P. Haloacid/dimethyl sulfoxide-catalyzed synthesis of symmetrical disulfides by oxidation of thiols. Tetrahedron Lett 2015; 56: 5578–82.
43 Dong WL, Huang GY, Li ZM, Zhao WG. A convenient method for the aerobic oxidation of thiols to disulfides. Phosphorus Sulfur Silicon 2009; 184: 2058–65.
44 Harpp DN, Smith RA. Reaction of trialkyl phosphites with organic trisulfides. Synthetic and mechanistic aspects. J Org Chem 1979; 44: 4140–44.
45 Hunter R, Caira M, Stellenboom N. Inexpensive, one-pot synthesis of unsymmetrical disulfides using 1-chlorobenzotriazole. J Org Chem 2006; 71: 8268–71.
46 Stellenboom N, Hunter R, Caira MR. One-pot synthesis of unsymmetrical disulfides using 1-chlorobenzotriazole as oxidant: Interception of the sulfenyl chloride intermediate. Tetrahedron 2010; 66: 3228–41.
47 Tanaka K, Ajiki K. Phosphine-free cationic rhodium (I) complex-catalyzed disulfide exchange reaction: convenient synthesis of unsymmetrical disulfides. Tetrahedron Lett 2004; 45: 5677–9.
48 Backer HJ, Kloosterziel H. Esters thiolsulfiniques. Recl Trav Chim Pays-Bas Et Belg 1954; 73: 129–39.
49 Colonna S, Gaggero N, Carrea G, Pasta P, Alphand V, Furstoss R. Enantioselective synthesis of tert-butyl tert-butanethiosulfinate catalyzed by cyclohexanone monooxygenase. Chirality 2001; 13: 40–2.
50 McNeil NM, McDonnell C, Hambrook M, Back TG. Oxidation of disulfides to thiolsulfinates with hydrogen peroxide and a cyclic seleninate ester catalyst. Molecules 2015; 20: 10748–62.
51 Kars MD, Iseri OD, Gunduz U, Ural AU, Arpaci F, Molnar J. Development of rational *in vitro* models for drug resistance in breast cancer and modulation of MDR by selected compounds. Anticancer Res 2006; 26: 4559–68.
52 Lipinski CA. Drug-like properties and the causes of poor solubility and poor permeability. J Pharmacol Toxicol Methods 2000; 44: 235–49.
53 OSIRIS Property Explorer [10 Jun 2016]. Available from: http://www.organic-chemistry.org/prog/peo/.
54 Shah STA, Khan KM, Fecker M, Voelter W. A novel method for the syntheses of symmetrical disulfides using CsF-Celite as a solid base. Tetrahedron Lett 2003; 44: 6789–91.
55 Hunter R, Caira M, Stellenboom N. Thiolsulfinate allicin from garlic: inspiration for a new antimicrobial agent. Ann N Y Acad Sci 2005; 1056: 234–41.

56 Lawson LD, Gardner CD. Composition, stability, and bioavailability of garlic products used in a clinical trial. J Agric Food Chem 2005; 53: 6254–61.
57 Fujisawa H, Suma K, Origuchi K, Kumagai H, Seki T, Ariga T. Biological and chemical stability of garlic-derived allicin. J Agric Food Chem 2008; 56: 4229–35.
58 Lipinski CA, Lombardo F, Dominy BW, Feeney PJ. Experimental and computational approaches to estimate solubility and permeability in drug discovery and development settings. Adv Drug Deliv Rev 2012; 64: 4–17.
59 Freeman F, Kodera Y. Garlic chemistry: stability of *S*-(2-propenyl)-2-propene-1-sulfinothioate (allicin) in blood, solvents, and simulated physiological fluids. J Agric Food Chem 1995; 43: 2332–8.
60 Elmore S. Apoptosis: a review of programmed cell death. Toxicol Pathol 2007; 35: 495–516.
61 Xu RH, Pelicano H, Zhou Y, Carew JS, Feng L, Bhalla KN, *et al.* Inhibition of glycolysis in cancer cells: a novel strategy to overcome drug resistance associated with mitochondrial respiratory defect and hypoxia. Cancer Res 2005; 65: 613–21.
62 Radde BN, Alizadeh-Rad N, Price SM, Schultz DJ, Klinge CM. Anacardic acid, salicylic acid, and oleic acid differentially alter cellular bioenergetic function in breast cancer cells. J Cell Biochem 2016; 117: 2521–32.
63 Cavallito CJ, Bailey JH, Buck JS. The antibacterial principle of *Allium sativum*. III. Its precursor and "Essential Oil of Garlic" 1. J Am Chem Soc 1945; 67: 1032–3.
64 Chen JS, Konopleva M, Andreeff M, Multani AS, Pathak S, Mehta K. Drug-resistant breast carcinoma (MCF-7) cells are paradoxically sensitive to apoptosis. J Cell Physiol 2004; 200: 223–34.
65 Janicke RU. MCF-7 breast carcinoma cells do not express caspase-3. Breast Cancer Res Treat 2009; 117: 219–21.
66 Leoni LM, Hamel E, Genini D, Shih H, Carrera CJ, Cottam HB, *et al.* Indanocine, a microtubule-binding indanone and a selective inducer of apoptosis in multidrug-resistant cancer cells. J Natl Cancer Inst 2000; 92: 217–24.
67 Park SY, Cho SJ, Kwon HC, Lee KR, Rhee DK, Pyo S. Caspase-independent cell death by allicin in human epithelial carcinoma cells: involvement of PKA. Cancer Lett 2005; 224: 123–32.
68 Miron T, Arditti F, Konstantinovski L, Rabinkov A, Mirelman D, Berrebi A, *et al.* Novel derivatives of 6-mercaptopurine: synthesis, characterization and antiproliferative activities of *S*-allylthio-mercaptopurines. Eur J Med Chem 2009; 44: 541–50.
69 Modem S, DiCarlo SE, Reddy TR. Fresh garlic extract induces growth arrest and morphological differentiation of MCF7 breast cancer cells. Genes Cancer 2012; 3: 177–86.
70 Prager–Khoutorsky M, Goncharov I, Rabinkov A, Mirelman D, Geiger B, Bershadsky AD. Allicin inhibits cell polarization, migration and division via its direct effect on microtubules. Cell Motil Cytoskeleton 2007; 64: 321–37.
71 Filomeni G, Rotilio G, Ciriolo MR. Cell signalling and the glutathione redox system. Biochem Pharmacol 2002; 64: 1057–64.
72 Marchetti P, Decaudin D, Macho A, Zamzami N, Hirsch T, Susin SA, *et al.* Redox regulation of apoptosis: Impact of thiol oxidation status on mitochondrial function. Eur J Immunol 1997; 27: 289–96.
73 Fath MA, Diers AR, Aykin-Burns N, Simons AL, Hua L, Spitz DR. Mitochondrial electron transport chain blockers enhance 2-deoxy-*D*-glucose induced oxidative stress and cell killing in human colon carcinoma cells. Cancer Biol Ther 2009; 8: 1228–36.
74 Pelicano H, Feng L, Zhou Y, Carew JS, Hileman EO, Plunkett W, *et al.* Inhibition of mitochondrial respiration a novel strategy to enhance drug-induced apoptosis in human leukemia cells by a reactive oxygen species-mediated mechanism. J Biol Chem 2003; 278: 37832–9.
75 Costantini P, Jacotot E, Decaudin D, Kroemer G. Mitochondrion as a novel target of anticancer chemotherapy. J Natl Cancer Inst 2000; 92: 1042–53.
76 Green DR, Reed JC. Mitochondria and apoptosis. Science 1998; 281: 1309.
77 Divakaruni A, Paradyse A, Ferrick D, Murphy A, Jastroch M. Analysis and interpretation of microplate-based oxygen consumption and pH data. Methods Enzymol 2013; 547: 309–54.
78 Pan J, Zhang Q, Liu Q, Komas SM, Kalyanaraman B, Lubet RA, *et al.* Honokiol inhibits lung tumorigenesis through inhibition of mitochondrial function. Cancer Prev Res 2014; 7: 1149–59.
79 Dranka BP, Benavides GA, Diers AR, Giordano S, Zelickson BR, Reily C, *et al.* Assessing bioenergetic function in response to oxidative stress by metabolic profiling. Free Radic Biol Med 2011; 51: 1621–35.
80 Laberge RM, Ambadipudi R, Georges E. P-glycoprotein (ABCB1) modulates collateral sensitivity of a multidrug resistant cell line to verapamil. Arch Biochem Biophys 2009; 491: 53–60.
81 Pluchino KM, Hall MD, Goldsborough AS, Callaghan R, Gottesman MM. Collateral sensitivity as a strategy against cancer multidrug resistance. Drug Resist Updat 2012; 15: 98–105.
82 Arora A, Seth K, Shukla Y. Reversal of P-glycoprotein-mediated multidrug resistance by diallyl sulfide in K562 leukemic cells and in mouse liver. Carcinogenesis 2004; 25: 941–9.
83 Höllt V, Kouba M, Dietel M, Vogt G. Stereoisomers of calcium antagonists which differ markedly in their potencies as calcium blockers are equally effective in modulating drug transport by P-glycoprotein. Biochem Pharmacol 1992; 43: 2601–8.
84 Hall MD, Handley MD, Gottesman MM. Is resistance useless? Multidrug resistance and collateral sensitivity. Trends Pharmacol Sci 2009; 30: 546–56.
85 Wu XJ, Kassie F, Mersch-Sundermann V. The role of reactive oxygen species (ROS) production on diallyl disulfide (DADS) induced apoptosis and cell cycle arrest in human A549 lung carcinoma cells. Mutat Res 2005; 579: 115–24.
86 Xiao D, Herman-Antosiewicz A, Antosiewicz J, Xiao H, Brisson M, Lazo JS, *et al.* Diallyl trisulfide-induced G2–M phase cell cycle arrest in human prostate cancer cells is caused by reactive oxygen species-dependent destruction and hyperphosphorylation of Cdc25C. Oncogene 2005; 24: 6256–68.
87 Zhao J, Zhang J, Yu M, Xie Y, Huang Y, Wolff DW, *et al.* Mitochondrial dynamics regulates migration and invasion of breast cancer cells. Oncogene 2013; 32: 4814–24.